Hydrogenation of the Two Diastereomers of the 66-Electron Linear Cluster $Ru_4(CO)_{10}[R^1C{=}C(H)C(H){=}NR^2]_2$. Hydrogen-Transfer Reactions and the Molecular Structure of the Only Isolable Diastereomer of the 64-Electron Butterfly Cluster $(\mu\text{-}H)_2Ru_4(CO)_8[CH_3C{=}C(H)C(H){=}N\text{-}i\text{-}Pr]_2$[1]

Wilhelmus P. Mul, Cornelis J. Elsevier,* Monique van Leijen, and Kees Vrieze

Anorganisch Chemisch Laboratorium, Universiteit van Amsterdam, J. H. van 't Hoff Instituut, Nieuwe Achtergracht 166, 1018 WV Amsterdam, The Netherlands

Wilberth J. J. Smeets and Anthony L. Spek

Vakgroep Kristal- en Structuurchemie, Universiteit te Utrecht, Padualaan 8, 3584 CH Utrecht, The Netherlands

Received October 9, 1991

The linear tetranuclear 66-electron clusters $Ru_4(CO)_{10}[R^1C{=}C(H)C(H){=}NR^2]_2$ (R^1, R^2 = CH_3, *i*-Pr (**3a**), CH_3, c-Hex (**3b**), C_6H_5, *i*-Pr (**3d**)), which consist of mixtures of diastereomers (*CC/AA*)-**3a,b,d** and (*CA/AC*)-**3a,b,d**, react in heptane solution at 90 °C with dihydrogen to yield only one of the two possible diastereomers of the tetranuclear 64-electron butterfly clusters $(\mu\text{-}H)_2Ru_4(CO)_8[R^1C{=}C(H)C(H){=}NR^2]_2$ ((*CC/AA*)-**5a,b,d**; ca. 45%), together with $H_4Ru_4(CO)_{12}$ (ca. 25%) and $R^1CH_2CH_2CH_2CH_2N(H)R^2$. Reaction of **3c** ($R^1$, R^2 = CH_3, *t*-Bu) with dihydrogen gave $H_4Ru_4(CO)_{12}$ and $CH_3CH_2CH_2CH_2N(H)$(*t*-Bu). These conversions proceed via the intermediacy of the dinuclear species $HRu_2(CO)_5[R^1C{=}C(H)C(H){=}NR^2]$ (**2**). The reactivity of the two diastereomers of **3a** toward dihydrogen differ. (*CA/AC*)-**3a** reacts with dihydrogen at 40 °C to give first two molecules of the dinuclear complex $HRu_2(CO)_5[CH_3C{=}C(H)C(H){=}N\text{-}i\text{-}Pr]$ (**2a**), which are subsequently converted into (*CC/AA*)-**5a**, $H_4Ru_4(CO)_{12}$, and $CH_3CH_2CH_2CH_2N(H)$(*i*-Pr), whereas (*CC/AA*)-**3a** has to be heated at 70 °C before conversion into **2a** and subsequent conversions take place. The compounds **5a,b,d** have been characterized by ^1H NMR, ^{13}C NMR, and IR spectroscopy, FI/FD mass spectrometry, and elemental analysis, and the X-ray crystal structure of (*CC/AA*)-**5a** has been determined. Crystals of (*CC/AA*)-**5a** are monoclinic, space group $P2_1/n$, with a = 10.852 (1) Å, b = 16.878 (2) Å, c = 15.476 (2) Å, β = 95.64 (1)°, Z = 4, and R = 0.029 (R_w = 0.031). Compound (*CC/AA*)-**5a** is an aggregate of two $Ru_2(CO)_4[CH_3C{=}C(H)C(H){=}N\text{-}i\text{-}Pr]$ units and two bridging hydrides, the presence of which was established chemically. The four ruthenium atoms in (*CC/AA*)-**5a** occupy a butterfly arrangement (ϕ = 137.05°) with two metal–metal bonds of normal length (ca. 2.82 Å) and three long bonds (3.12–3.14 Å). The monoazadienyl ligands in (*CC/AA*)-**5a** adopt, as in **2** and **3**, the bridging seven-electron-donating $\sigma(N)\text{-}\sigma(C)\text{-}\eta^2(C{=}C)\text{:}\eta^2(C{=}N)$ coordination mode, and the eight CO ligands are all terminally bonded. On the basis of the structural data for (*CC/AA*)-**5a**, the instability of the other diastereomers (*CA/AC*)-**5a–d** and of (*CC/AA*)-**5c** (R^2 = *t*-Bu) is discussed. Several hydrogenation and H-transfer reactions involving the monoazadienyl ligand have been observed. For instance, reaction of **3a–d** at 90 °C under an atmosphere of H_2/CO (9:1) gives $Ru_2(CO)_6[R^1C{=}C(H)CH_2NR^2]$ (**1a–d**; 60–80%). Reaction of **5a,b,d** with CO at 90 °C also gives **1a,b,d** in nearly quantitative yield. Both reactions probably proceed via $HRu_2(CO)_5[R^1C{=}C(H)C(H){=}NR^2]$ (**2**) and $HRu_2(CO)_6[R^1C{=}C(H)C(H){=}NR^2]$ (**6**), since at ambient temperature **2c** rapidly takes up one CO ligand to give **6c**, which contains a five-electron-donating $\sigma(N)\text{-}\sigma(C)\text{-}\eta^2(C{=}C)$-bonded monoazadienyl ligand, which can be thermally isomerized to give **1c**. During this conversion, the hydride in **6** is transferred to the imine C atom of the monoazadienyl ligand. Conversion of **6c** into **1c**, however, only takes place at a reasonable rate at 80 °C under an atmosphere of CO; otherwise conversion into **3c** dominates. On silica, **6** isomerizes into $Ru_2(CO)_6[R^1CC(H)C(H)N(H)R^2]$ (**7**). This isomerization takes place stereospecifically, as only one diastereomer of **7** is formed. Thermal reaction of $Ru_2(CO)_6[CH_2CC(H)C(H){=}NR^2]$ (**4a,c**) with dihydrogen at 100 °C gives **1a** and **3c**, respectively. These conversions probably take place via **6a,c**. The deviating reactivity of **6** with R^2 = *t*-Bu (**6c**) compared to that with R^2 = *i*-Pr or c-Hex (**6a,b**) and the intermediacy of this crucial compound during thermal reactions of $Ru_3(CO)_{12}$ with monoazadienes $R^1C(H){=}C(H)C(H){=}NR^2$ are discussed.

Introduction

By definition, diastereomers have different physical and chemical properties. Physical differences make them spectroscopically distinguishable and separable by techniques such as crystallization or chromatography. Chemical differences are reflected particularly in regio- and stereoselective synthesis. For instance, the reaction rates of diastereomeric organometallic complexes toward H_2 may differ markedly, as has amply been demonstrated by, among others, Halpern and Bosnich.[2]

As has already been elaborated previously, the linear tetranuclear clusters $Ru_4(CO)_{10}[R^1\text{-}C{=}C(H)C(H){=}NR^2]_2$ (**3**) exist as mixtures of two diastereomers.[3,4] The clusters **3**, which contain two β-metalated monoazadien-4-yl ligands (MAD-yl), are formed in good to excellent yields during thermal reactions of $Ru_3(CO)_{12}$ with $R^1C(H){=}C(H)C\text{-}$

(1) Reactions and Monoazadienes with Metal Carbonyl Complexes. 10. Part 9: reference 4.

(2) (a) Halpern, J. *Inorg. Chim. Acta* **1981**, *50*, 11. (b) Bosnich, B.; Fryzuk, M. D. *Top. Stereochem.* **1981**, *12*, 119.

(3) Polm, L. H.; Mul, W. P.; Elsevier, C. J.; Vrieze, K.; Chrisophersen, M. J. N.; Stam, C. H. *Organometallics* **1988**, *8*, 423.

(4) Mul, W. P.; Elsevier, C. J.; Ernsting, J. M.; de Lange, W. G. J.; van Straalen, M. D. M.; Vrieze, K.; de Wit, M.; Stam, C. H. *J. Am. Chem. Soc.*, submitted for publication.

0276-7333/92/2311-1877$03.00/0

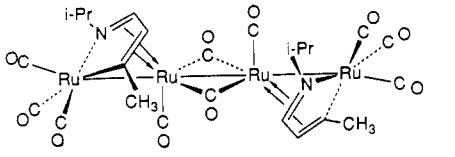

trans-(CA/AC)-**3a**

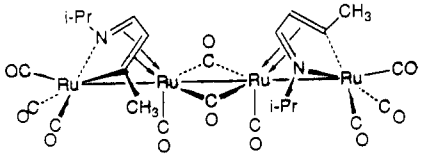

cis-(CC/AA)-**3a**

Figure 1. The two diastereomers of **3a**.

(H)=NR^2 (R^1,R^2-MAD).[3,5,6] The dinuclear complexes $Ru_2(CO)_6[R^1C{=}C(H)CH_2NR^2]$ (**1**) and $HRu_2(CO)_5[R^1C{=}C(H)C(H){=}NR^2]$ (**2**) were shown to be intermediates during the formation of **3**.[6,7] For **3a** (R^1, R^2 = CH_3, *i*-Pr) the diastereomers have been separated by HPLC on a preparative scale.[4] Figure 1 shows schematic representations of the solid-state structures of these diastereomers, *trans*-(*CA/AC*)-**3a** and *cis*-(*CC/AA*)-**3a**, as found in the crystal structures. At ambient temperature, however, rapid cis/trans isomerization takes place in solution for both the *CA/AC* and *CC/AA* diastereomers of **3a**, whereas also in the solid state each diastereomer may adopt the cis or trans conformation.[4] At elevated temperatures in solution interconversion of the *CA/AC* and *CC/AA* diastereomers occurs intramolecularly.[4]

Several ruthenium carbonyl complexes have been shown to be useful homogeneous catalysts for hydrogenation, dehydrogenation, hydroformylation, carbonylation, and hydrogen transfer and exchange reactions.[8] In the course of our study aimed at a better understanding of the reactivity of **3** and its potential for such catalytic reactions, we investigated reactions of **3** with syngas and its components, H_2 and CO. Moreover, since a MAD-yl ligand contains both unsaturated C=N and C=C moieties, both diastereomers of tetranuclear **3**, which contain two such ligands, constitute interesting models for which chemoselectivity in the hydrogenation of C=N and C=C moieties can be studied.

This is the first of two papers reporting on the results of reactions of **3** with H_2 and/or CO. It will be shown that (*CA/AC*)-**3a** and (*CC/AA*)-**3a** have different kinetic barriers for hydrogenation and that only one of two possible geometric isomers of the product, a tetranuclear dihydrido cluster, is obtained selectively. Furthermore, the C=N moiety of the MAD-yl ligand may be reduced chemoselectively by H-transfer from the metal core to either the imine C or N atom. The actual pathway depends on how the hydride intermediate is activated. In the next paper we will concentrate on the various reactions of **3a** with CO, including directable regioselective C–H activation processes.[9]

Experimental Section

Materials and Apparatus. ^{1}H, ^{2}H, and $^{13}C\{^1H\}$ NMR spectra were obtained on Bruker AC100 and WM250 spectrometers. The ^{13}C NMR spectra were recorded using an APT pulse sequence. NMR experiments under gas pressures up to 20 bar were carried out by using a home-built apparatus consisting of a Ti/Al/V pressure head and a 10-mm external diameter and 8.4-mm internal diameter sapphire NMR tube, suitable for measurements under 1–140 bar of gas pressures.[10] IR spectra were recorded with Perkin-Elmer 283 and Nicolet 7199 B FT-IR spectrophotometers using matched NaCl solution cells of 0.5-mm path length. Field desorption (FD) and field ionization (FI) mass spectra[11] were obtained with a Varian MAT-711 double-focusing mass spectrometer with a combined EI/FI/FD source, fitted with a 10-μm tungsten-wire FD emitter containing carbon microneedles with an average length of 30 μm, using emitter currents of 0–15 mA. Elemental analyses were carried out by the Elemental Analysis Section of the Institute for Applied Chemistry, TNO, Zeist, The Netherlands. Solvents were carefully dried and distilled prior to use. All syntheses were carried out under an atmosphere of dry nitrogen, unless stated otherwise, by using Schlenk techniques. Silica gel for column chromatography (Kieselgel 60, 70–230 mesh, E. Merck, Darmstadt, Germany) was dried before use. The monoazadienes (R^{1}C(H)=C(H)C(H)=NR^2; R^1,R^2-MAD)[5] have been prepared according to standard procedures.[12] The compounds $HRu_2(CO)_5[C_6H_5C{=}C(H)C(H){=}N\text{-}i\text{-}Pr]$ (**2d**), $Ru_4(CO)_{10}[R^1C{=}C(H)C(H){=}NR^2]_2$ (R^1, R^2 = CH_3, *i*-Pr (**3a**), CH_3, c-Hex (**3b**), CH_3, *t*-Bu (**3c**), C_6H_5, *i*-Pr (**3d**)), and $Ru_2(CO)_6[CH_2CC(H)C(H){=}NR^2]$ (R^2 = *i*-Pr (**4a**), *t*-Bu (**4c**)) were synthesized as described before.[3,6,13] The *CA/AC* and *CC/AA* diastereomers of **3a** were separated by preparative HPLC as described.[4]

Synthesis of $H_2Ru_4(CO)_8[R^1C{=}C(H)C(H){=}NR^2]_2$ (R^1, R^2 = CH_3, *i*-Pr (5a), CH_3, c-Hex (5b), C_6H_5 *i*-Pr (5d)). Dihydrogen was bubbled through a solution or suspension of $Ru_4(CO)_{10}[R^1C{=}C(H)C(H){=}NR^2]_2$ (**3a,b,d**; 0.5 mmol) in 50 mL of heptane at 90 °C. The reaction was monitored by IR spectroscopy and stopped when the 1770-cm^{-1} band belonging to **3** had disappeared (2–4 h). The purple solution was concentrated to 10 mL and the dissolved organometallic components separated by column chromatography. Elution with hexane gave two fractions. The first pale yellow fraction contained a small amount of **1a,b,d** (≤5%). The second yellow fraction was identified as $H_4Ru_4(CO)_{12}$ (ca. 25%) by IR spectroscopy (ν(CO) in hexane: 2077 (s), 2063 (vs), 2021 (s) cm^{-1} (lit.[15] (in cyclohexane): 2081 (s), 2067 (vs), 2030 (m), 2024 (s), 2009 (w) cm^{-1}), ^{1}H NMR spectroscopy (δ(hydride) in $CDCl_3$: −17.81 ppm (lit.:[15] −17.98 ppm)), and FD mass spectroscopy (found *m/e* 744; calcd M_r 744).[14] Subsequent elution with hexane/dichloromethane (9:1) afforded a purple fraction containing $H_2Ru_4(CO)_8[R^1C{=}C(H)C(H){=}NR^2]_2$ (**5a,b,d**; ca. 45%). Further elution with dichloromethane produced a small

(5) MAD is used as an acronym for monoazadienes in general. In this paper we will use R^1,R^2-MAD when *N*-alkyl-(*E*)-crotonaldimines (CH_3C(H)=C(H)C(H)=NR^2) or *N*-alkyl-(*E*)-cinnamaldimines (C_6H_5C(H)=C(H)C(H)=NR^2) are meant. Metalated at C_β, these ligands form the formally monoanionic monoazadien-4-yl (R^1,R^2-MAD-yl) ligand R^{1}C$^-$=C(H)C(H)=NR^2. Subscripts of the atoms refer to R^{1}C(H)$_\beta$=C(H)$_\alpha$C(H)$_{im}$=NR^2.

(6) Mul, W. P.; Elsevier, C. J.; Polm, L. H.; Vrieze, K.; Zoutberg, M.; Heijdenrijk, D.; Stam, C. H. *Organometallics* **1991**, *10*, 2247.

(7) Spek, A. L.; Duisenberg, A. J. M.; Mul, W. P.; Beers, O. C. P.; Elsevier, C. J. *Acta Crystallogr.* **1991**, *C47*, 297.

(8) See for example: (a) Bennett, M. A.; Matheson, T. W. In *Comprehensive Organometallic Chemistry*; Wilkinson, G., Stone, F. G. A., Abel, E. W., Eds.; Pergamon: Oxford, U.K., 1982; Vol. 4, Chapter 32.9, and references cited therein. (b) Halpern, J.; James, B. R.; Kemp, A. L. W. *J. Am. Chem. Soc.* **1966**, *88*, 5142. (c) Halpern, J.; Farrod, J. F.; James, B. R. *J. Am. Chem. Soc.* **1966**, *88*, 5150. (d) James, B. R. *Inorg. Chim. Acta* **1970**, 73. (e) Strathdee, G.; Given, R. M. *Can. J. Chem.* **1975**, *53*, 106. (f) Byerley, J. J.; Rempel, G. L.; Takebe, N.; James, B. R. *J. Chem. Soc., Chem. Commun.* **1975**, 718. (g) Pruett, R. L. *Adv. Organomet. Chem.* **1979**, *17*, 1. (h) James, B. R. *Adv. Organomet. Chem.* **1979**, *17*, 319. (i) Halpern, J. *Pure Appl. Chem.* **1987**, *59*, 173. (j) Bhadura, S.; Sharma, K. *J. Chem. Soc., Chem. Commun.* **1988**, 173. (k) Takaya, H.; Ohta, T.; Masma, K.; Noyori, R. *Pure Appl. Chem.* **1990**, *62*, 1135.

(9) Mul, W. P.; Elsevier, C. J.; Vrieze, K.; Smeets, W. J. J.; Spek, A. L. *Organometallics*, following article in this issue.

(10) Roe, D. C. *J. Magn. Reson.* **1985**, *63*, 388.

(11) Schulten, H. R. *Int. J. Mass Spectrosc. Ion Phys.* **1979**, *32*, 97.

(12) Barany, H. C.; Braude, E. A.; Pianka, M. *J. Chem. Soc.* **1949**, 1898.

(13) Polm, L. H.; Elsevier, C. J.; Mul, W. P.; Vrieze, K.; Christophersen, M. J. N.; Muller, F.; Stam, C. H. *Polyhedron* **1988**, *7*, 2521.

(14) Based on the peak of the isotopic pattern of the molecular ion that corresponded to ^{101}Ru (calculated value in parentheses).

(15) Knox, S. A. R.; Koepke, J. W.; Andrews, M. A.; Kaesz, H. D. *J. Am. Chem. Soc.* **1975**, *97*, 3942.

amount of starting material **3a,b,d** (≤5%). Crystals of **5a**, suitable for X-ray diffraction, were obtained by slowly evaporating pentane into a concentrated dichloromethane solution. Anal. Found (calcd) for $C_{22}H_{26}N_2O_8Ru_4$ (**5a**): C, 31.02 (31.06); H, 3.11 (3.08); N, 3.25 (3.29). FI-MS: found m/e 850; calcd M_r 850. Anal. Found (calcd) for $C_{28}H_{34}N_2O_8Ru_4$ (**5b**): C, 36.01 (36.13); H, 3.74 (3.68); N, 2.95 (3.01). FD-MS: found m/e ~928; calcd M_r 930. Anal. Found (calcd) for $C_{32}H_{30}N_2O_8Ru_4$ (**5d**): C, 39.11 (39.43); H, 2.98 (3.10); N, 2.88 (2.87). FD-MS: found m/e ~973; calcd M_r 974.[14]

When $Ru_4(CO)_{10}[CH_3C{=}C(H)C(H){=}N\text{-}t\text{-}Bu]_2$ (**3c**) was used as the starting material and reacted with H_2 as described above, the only inorganic product obtained after 4 h was $H_4Ru_4(CO)_{12}$ (IR, ^1H NMR).

Isolation and Identification of Organic Hydrogenation Products. A solution of **3a** or **3c** (0.05 mmol) in 2 mL of C_6D_6 was reacted with H_2 as described above. After the reaction mixture was cooled to ambient temperature, the volatile organic components were isolated by distillation into a small cold (−80 °C) Schlenk tube under reduced pressure. ^1H NMR and GC–MS studies showed the presence of $CH_3CH_2CH_2CH_2N(H)R^2$. $CH_3CH_2CH_2CH_2N(H)(i\text{-}Pr)$: ^1H NMR (δ, in C_6D_6 (multiplicity, integral)) 2.64 (sept, 1 H), 2.46 (m, 2 H), 1.34 (m, 4 H), 0.98 (d, 6 H), 0.89 (m, 3 H); GC–MS (m/e (%, fragment)) 115 (8, $M^{\bullet+}$), 100 (62, $M^{\bullet+} - CH_3$), 72 (100, $M^{\bullet+} - i\text{-}Pr$). $CH_3CH_2CH_2CH_2N(H)(t\text{-}Bu)$: ^1H NMR (δ, in C_6D_6 (multiplicity, integral)) 2.47 (m, 2 H), 1.36 (m, 4 H), 1.02 (s, 9 H), 0.90 (m, 3 H); GC–MS (m/e (%, fragment)) 115 (8, $M^{\bullet+}$), 100 (62, $M^{\bullet+} - CH_3$).

Reaction of $Ru_4(CO)_{10}[R^1C{=}C(H)C(H){=}NR^2]_2$ (R^1, R^2 = CH_3, *i*-Pr (3a), CH_3, c-Hex (3b), CH_3, *t*-Bu (3c), C_6H_5, *i*-Pr (3d)) with H_2/CO. A solution (or suspension) of $Ru_4(CO)_{10}[R^1C{=}C(H)C(H){=}NR^2]_2$ (R^1, R^2 = CH_3, *i*-Pr (**3a**), CH_3, c-Hex (**3b**), CH_3, *t*-Bu (**3c**), C_6H_5, *i*-Pr (**3d**); 0.5 mmol) in 50 mL of heptanes was stirred at 90 °C under an atmosphere of H_2/CO (250-mL Schlenk tube; ratio 9:1). The initial red color of the solution gradually changed to yellow/orange. The reaction was followed by IR spectroscopy and stopped when the IR bands originating from the bridging CO ligands of **3** (~1770 cm^{-1}) had disappeared (1–2 h). The solution was concentrated to 5 mL and cooled to −80 °C, which resulted in the precipitation of small amounts of $H_4Ru_4(CO)_{12}$ and unreacted starting material. After filtration the solution was purified by chromatography on silica. Elution with hexane afforded a light yellow band of $Ru_2(CO)_6[R^1C{=}C(H)CH_2NR^2]$ (**1a–d**; 60–80%) and a less mobile yellow band of $Ru_2(CO)_6[CH_2CC(H)C(H){=}NR^2]$ (**4a–c**; ≤10%). In the case with R^2 = *t*-Bu subsequent elution with hexane/diethyl ether (4:1) gave a small amount of $Ru_2(CO)_6[CH_3CC(H)C(H)N(H)(t\text{-}Bu)]$ (**7c**; ca. 5%). Anal. Found (calcd) for $C_{14}H_{15}NO_6Ru_2$ (**1c**): C, 33.47 (33.94); H, 2.87 (3.05); N, 2.70 (2.83). FD-MS: found, m/e 495; calcd M_r 495.[14]

Thermal Reaction of $H_2Ru_4(CO)_8[R^1C{=}C(H)C(H){=}NR^2]_2$ (R^1, R^2 = CH_3, *i*-Pr (5a), CH_3, c-Hex (5b), C_6H_5, *i*-Pr (5d)) with CO. A solution of $H_2Ru_4(CO)_8[R^1C{=}C(H)C(H){=}NR^2]_2$ (**5a,b,d**; 0.1 mmol) in 25 mL of heptane was stirred at 90 °C under an atmosphere of CO. The purple color slowly changed to yellow. Conversion into $Ru_2(CO)_6[R^1C{=}C(H)CH_2NR^2]$ (**1a,b,d**), which was nearly quantitative, was completed after about 2 h. The products were isolated as described before.[6]

Reaction of $Ru_2(CO)_6[CH_2CC(H)C(H){=}N\text{-}i\text{-}Pr]$ (4a) with H_2. A solution of $Ru_2(CO)_6[CH_2CC(H)C(H){=}N\text{-}i\text{-}Pr]$ (**4a**; 0.2 mmol) in 25 mL of heptane was stirred at 100 °C under an atmosphere of H_2. The reaction was stopped after about 0.5 h, when in the IR spectrum the bands belonging to **4a** were replaced by those of $Ru_2(CO)_6[CH_3CC(H)CH_2N\text{-}i\text{-}Pr]$ (**1a**). The crude reaction mixture was purified by column chromatography. Elution with hexane afforded a pale yellow fraction containing **1a** in about 75% yield.

Reaction of $Ru_2(CO)_6[CH_2CC(H)C(H){=}N\text{-}t\text{-}Bu]$ (4c) with H_2. A solution of $Ru_2(CO)_6[CH_2CC(H)C(H){=}N\text{-}t\text{-}Bu]$ (**4c**; 0.5 mmol) in 25 mL of heptane was stirred at reflux under an atmosphere of H_2. The reaction was carefully monitored by IR spectroscopy performed on small samples which were taken from the reaction mixture at regular intervals. The reaction was stopped when the absorption bands belonging to $Ru_4(CO)_{10}[CH_3C{=}C(H)C(H){=}N\text{-}t\text{-}Bu]_2$ (**3c**) had reached a maximum intensity (about 3 h). Then the solvent was removed under vacuum and the nonvolatile components were separated by column chromatography on silica. Elution with hexane gave a broad yellow band containing both $H_4Ru_4(CO)_{12}$ and $Ru_2(CO)_6[CH_3C{=}C(H)CH_2N\text{-}t\text{-}Bu]$ (**1c**; ca. 5%) and, furthermore, some unreacted starting material **4c**. Further elution with hexane/diethyl ether (1:1) gave a mixture of **3c** and $Ru_2(CO)_6[CH_3CC(H)C(H)N(H)(t\text{-}Bu)]$ (**7c**). This second fraction was further purified by column chromatography on a second column of silica. A yellow band of **7c** (15%) was eluted by using hexane/dichloromethane (10:1) as the eluent. With dichloromethane as the eluent an orange/red band was obtained containing **3c** in a yield of 60%.

Synthesis of $HRu_2(CO)_6[CH_3C{=}C(H)C(H){=}N\text{-}t\text{-}Bu]$ (6c). A solution of $Ru_4(CO)_{10}[CH_3C{=}C(H)C(H){=}N\text{-}t\text{-}Bu]_2$ (**3c**; 0.5 mmol) in 20 mL of benzene was stirred at 50 °C under an atmosphere of H_2/CO (9:1) in a sealed 250-mL Schlenk tube for 3 h. After this period the solvent was removed under vacuum and the brown residue extracted twice with 3 mL of cold hexane (0 °C). The solution was evaporated to leave an orange-brown oil, which was dissolved in ethanol and cooled to −80 °C, affording yellow crystals of $HRu_2(CO)_6[CH_3C{=}C(H)C(H){=}N\text{-}t\text{-}Bu]$ (**6c**) in about 50% yield (based on converted **3c**). Unreacted **3c** (40%) was recovered from the solid material remaining after extraction.[6] Anal. Found (calcd) for $C_{14}H_{15}NO_6Ru_2$ (**6c**): C, 34.32 (33.94); H, 3.13 (3.05); N, 2.68 (2.83). FD-MS: found, m/e 495; calcd, M_r 495.[14]

Synthesis of $HRu_2(CO)_6[C_6H_5C{=}C(H)C(H){=}N\text{-}i\text{-}Pr]$ (6d). A solution of $HRu_2(CO)_5[C_6H_5C{=}C(H)C(H){=}N\text{-}i\text{-}Pr]$ (**2d**) in 25 mL of hexane was stirred under an atmosphere of CO for 5 min. During this period the characteristic ν(CO) pattern of **2d** had disappeared and was replaced by that of $HRu_2(CO)_6[C_6H_5C{=}C(H)C(H){=}N\text{-}i\text{-}Pr]$ (**6d**). The conversion was virtually quantitative. The solvent was removed under vacuum, yielding pure orange **6d**. Anal. Found (calcd) for $C_{18}H_{15}NO_6Ru_2$ (**6d**): C, 39.88 (39.78); H, 2.96 (2.78); N, 2.70 (2.58). FD-MS: found, m/e 543; calcd, M_r 543.[14]

Thermolysis of $HRu_2(CO)_6[CH_3C{=}C(H)C(H){=}N\text{-}t\text{-}Bu]$ (6c). A solution of $HRu_2(CO)_6[CH_3C{=}C(H)C(H){=}N\text{-}t\text{-}Bu]$ (**6c**; 0.2 mmol) in 30 mL of heptane was stirred at 75 °C for 1 h. During this period conversion took place to give $Ru_4(CO)_{10}[CH_3C{=}C(H)C(H){=}N\text{-}t\text{-}Bu]_2$ (**3c**; ca. 90%) and a small amount of $Ru_2(CO)_6[CH_3C{=}C(H)CH_2N\text{-}t\text{-}Bu]$ (**1c**; ≤10%).

When a solution of **6c** in heptanes was placed under an atmosphere of CO and stirred at 80 °C for 4 h, **1c** was obtained in nearly quantitative yield.

Thermolysis of $HRu_2(CO)_6[C_6H_5C{=}C(H)C(H){=}N\text{-}i\text{-}Pr]$ (6d). A solution of $HRu_2(CO)_6[C_6H_5C{=}C(H)C(H){=}N\text{-}i\text{-}Pr]$ (**6d**; 0.2 mmol) in 25 mL of hexane was stirred at reflux for 5 min. During this period complete conversion into $Ru_2(CO)_6[CH_3C{=}C(H)CH_2N\text{-}i\text{-}Pr]$ (**1d**) took place. The product could be isolated as described before.[6]

Reaction of $HRu_2(CO)_6[CH_3C{=}C(H)C(H){=}N\text{-}t\text{-}Bu]$ (6c) with $CH_3C(H){=}C(H)C(H){=}N\text{-}t\text{-}Bu$. A solution of $HRu_2(CO)_6[CH_3C{=}C(H)C(H){=}N\text{-}t\text{-}Bu]$ (**6c**; 0.2 mmol) in 30 mL of heptane was stirred at 70 °C in the presence of an excess of $CH_3C(H){=}C(H)C(H){=}N\text{-}t\text{-}Bu$ (1 mmol) for 30 min. The resulting reaction mixture was filtered over silica and examined by IR and ^1H NMR spectroscopy and FI mass spectrometry. It was found that nearly quantitative conversion into $Ru_2(CO)_6[CH_2CC(H)C(H){=}N\text{-}t\text{-}Bu]$ (**4c**) had taken place. This product could be isolated as described before.[13]

Conversion of $HRu_2(CO)_6[R^1C{=}C(H)C(H){=}NR^2]$ (R^1, R^2 = CH_3, *t*-Bu (6c), C_6H_5, *i*-Pr (6d)) into $Ru_2(CO)_6[R^1CC(H)C(H)N(H)R^2]$ (7c,d). A solution of $HRu_2(CO)_6[R^1C{=}C(H)C(H){=}NR^2]$ (**6c,d**) in 20 mL of hexane/dichloromethane (1:1) was stirred in the presence of a small amount of silica (2 g) for 1 h. After this period the silica was filtered off and washed with 5 mL of dichloromethane. The combined filtrate and washing was concentrated, affording $Ru_2(CO)_6[R^1CC(H)C(H)N(H)R^2]$ (**7c,d**) in nearly quantitative yield. Orange-yellow microcrystalline **7c** or **7d** was obtained by cooling a concentrated hexane solution to −80 °C. Anal. Found (calcd) for $Ru_2C_{14}H_{15}NO_6$ (**7c**): C, 33.77 (33.94); H, 3.00 (3.05); N, 2.58 (2.83). FD-MS: found, m/e 495; calcd, M_r 495.[14] Anal. Found (calcd) for $C_{18}H_{15}NO_6Ru_2$ (**7d**): C, 39.54 (39.78); H, 2.66 (2.78); N, 2.68 (2.58). FD-MS: found, m/e 543; calcd, M_r 543.[14]

Crystal Structure Determination of $(\mu\text{-}H)_2Ru_4(CO)_8[CH_3C{=}C(H)C(H){=}N\text{-}i\text{-}Pr]_2$ (5a). Data were collected on an

Table I. Crystal Data for 5a

chem formula	$C_{22}H_{26}N_2O_8Ru_4$	β	95.64 (1)°
mol wt	850.74	D_{calcd}	2.003 g cm^{-3}
space group	$P2_1/n$	V	2820.9 (6) Å^3
Z	4	$F(000)$	1648
a	10.852 (1) Å	μ(Mo Kα)	21.1 cm^{-1}
b	16.878 (2) Å		
c	15.476 (2) Å		

Enraf-Nonius CAD4F diffractometer (Mo Kα (Zr filtered); λ = 0.710 73 Å; 295 K) for a dark purple block-shaped crystal (0.62 × 0.90 × 0.90 mm) glued on a glass fiber (θ_{max} = 27.5°; $\omega/2\theta$ scan, $\Delta\omega$ = (0.60 + 0.35 tan θ)°; h = −13 to +14, k = −21 to 0, l = −20 to 0). Unit cell parameters were derived from the setting angles of 12 SET4 reflections ($\theta \approx 12°$). A total of 6457 reflections were scanned and their intensities corrected for Lp and absorption (DIFABS,[16] corrections 0.87–1.18). The structure was solved with Patterson techniques (SHELXS-86)[17] and refined on F with anisotropic weighted least squares (SHELX-76).[18] Hydrogen atoms H(1), H(2), H(31), H(41), H(101), and H(111) were located from a difference map and their positions refined (with a restraint on the Ru–H bond distance). All other hydrogen atoms were introduced at calculated positions and refined riding on their carrier atom (C–H = 0.98 Å) with one common isotropic U parameter. A difference map calculated at this stage showed residual peaks that were interpreted as a Ru_4 core in another orientation. They were included in a disorder model affecting the Ru_4 atoms only (0.98:0.02). A few too-strong reflections were left out of the final refinement. Convergence was reached at R = 0.029 (R_w = 0.031; $w^{-1} = \sigma^2(F)$; S = 1.80; 375 parameters; 5621 reflections with $I > 2.5\sigma(I)$). A final difference map showed no excursions outside $-0.51 < \Delta\rho < 0.54$ e Å^{-3}. Scattering factors were taken from ref 19, corrected for anomalous dispersion.[20] Geometric calculations, including the illustration, were done with PLATON[21] on a microVAX-II cluster. Crystal data are given in Table I.

Results

Reaction of $Ru_4(CO)_{10}[R^1C{=}C(H)C(H){=}NR^2]_2$ (3a–d) with H_2. When dihydrogen is bubbled through a solution of the 66-electron linear cluster $Ru_4(CO)_{10}[R^1C{=}C(H)C(H){=}NR^2]_2$ (R^1, R^2 = CH_3, *i*-Pr (**3a**), CH_3, c-Hex (**3b**), C_6H_5, *i*-Pr (**3d**); mixtures of *CC/AA* and *CA/AC* diastereomers) in heptane for 2–4 h at 90 °C, the two tetranuclear compounds $H_2Ru_4(CO)_8[R^1C{=}C(H)C(H){=}NR^2]_2$ (**5a,b,d**; ca. 45%) and $H_4Ru_4(CO)_{12}$ (ca. 25%) are obtained after chromatographic fractionation of the reaction mixture on silica (eq 1). After isolation of the

$$\underset{\textbf{3a,b,d}}{Ru_4(CO)_{10}[R^1C{=}C(H)C(H){=}NR^2]_2} + H_2 \xrightarrow{90\ °C} \underset{\textbf{5a,b,d}}{H_2Ru_4(CO)_8[R^1C{=}C(H)C(H){=}NR^2]_2} + H_4Ru_4(CO)_{12} + R^1CH_2CH_2CH_2N(H)R^2 \quad (1)$$

	R^1	R^2
a	CH_3	*i*-Pr
b	CH_3	c-Hex
c	CH_3	*t*-Bu
d	C_6H_5	*i*-Pr

volatile organic products from the reaction of **3a** with dihydrogen (performed in C_6D_6) by distillation, ^{1}H NMR spectroscopy showed the presence of $CH_3CH_2CH_2CH_2N(H)$(*i*-Pr), which was confirmed by GC–MS. This saturated secondary amine has been formed by complete hydrogenation of the MAD-yl ligand.

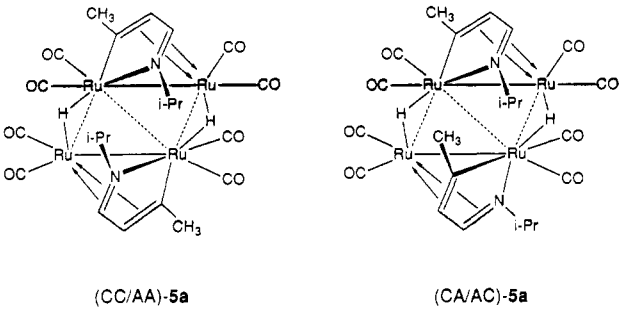

Figure 2. The two possible diastereomers of **5a**.

Due to the presence of two intrinsically asymmetric azaruthenacycles in **5**, two diastereomers, (*CA/AC*)-**5** and (*CC/AA*)-**5**, can be envisaged (Figure 2).[22] However, both in solution (NMR) and in the solid state (X-ray) only one of the two possible geometric isomers of this new 64-electron butterfly cluster, (*CC/AA*)-**5a,b,d**, is observed after completion of the reaction.[23] The isolated *CC/AA* diastereomer of **5a,b,d** is stable under the applied reaction conditions; hence, formation of $H_4Ru_4(CO)_{12}$ and $R^1CH_2CH_2CH_2N(H)R^2$ is not the result of partial decomposition of (*CC/AA*)-**5a,b,d**.

Hydrogenation of $Ru_4(CO)_{10}[CH_3C{=}C(H)C(H){=}N$-*t*-Bu$]_2$ (**3c**) under similar conditions only produced $H_4Ru_4(CO)_{12}$ and $CH_3CH_2CH_2CH_2N(H)$(*t*-Bu). Formation of $H_2Ru_4(CO)_8[CH_3C{=}C(H)C(H){=}N$-*t*-Bu$]_2$ (**5c**) was not observed.

Mechanistic Aspects of Hydrogenation of the Two Diastereomers of $Ru_4(CO)_{10}[R^1C{=}C(H)C(H){=}N$-*i*-Pr$]_2$ (3a). In search of possible reaction intermediates of (*CA/AC*)-**5a**, the reaction of **3a** with H_2 was followed with ^{1}H NMR spectroscopy using a pressurizable sapphire NMR tube.[10] To this end an approximately equimolar mixture of (*CA/AC*)-**3a** and (*CC/AA*)-**3a** in C_6D_6 under 10 bar of molecular hydrogen was heated stepwise between 20 and 70 °C. Several reaction stages were observed. First, at 40 °C, slow conversion of (*CA/AC*)-**3a** into a new species takes place which contains, as exemplified by its ^{1}H NMR characteristics, a 7e-donating monoazadienyl (MAD-yl) ligand ($\delta(H_{im})$ 6.12 ppm; $\delta(H_\alpha)$ 5.45 ppm)[5] and a hydride (−9.77 ppm). The ^{1}H NMR and IR[24] data as well as the

(16) Walker, N.; Stuart, D. *Acta Crystallogr.* **1983**, *A39*, 158.
(17) Sheldrick, G. M. SHELXS86: Program for Crystal Structure Solution; University of Göttingen: Göttingen, Germany, 1986.
(18) Sheldrick, G. M. SHELX76: Crystal Structure Analysis Package; University of Cambridge: Cambridge, England, 1976.
(19) Cromer, D. T.; Mann, J. B. *Acta Crystallogr.* **1968**, *A24*, 321.
(20) Cromer, D. T.; Liberman, D. *J. Chem. Phys.* **1970**, *53*, 1891.
(21) Spek, A. L. The Euclid Package. In *Computational Crystallography*; Sayre, D., Ed., Clarendon Press: Oxford, England, 1982; p 528.

(22) Hereby we assume a flying motion of the wingtips of the butterfly cluster to be facile, resulting in the energetically most favored geometry; otherwise four diastereomers would have to be considered. Such a dynamic process has, for instance, been observed for $Ru_4(CO)_8$(*i*-Pr-DAB)$_2$.[36a]

(23) The configurations of the chiral, cyclometalated ruthenium atoms in **5**, Ru(2) and Ru(3), have been determined according to the Brown–Cook–Sloan modification of the Cahn–Ingold–Prelog rules,[23a–c] which have recently been recommended by IUPAC.[23d] Hereby it is assumed that there are no (metal–metal) bonds between Ru(1) and Ru(2), Ru(2) and Ru(3), and Ru(3) and Ru(4) in **5**. Throughout this paper the official stereochemical descriptors for the chiral ruthenium atoms, i.e. *OC*-6-33-*C* and *OC*-6-33-*A*, will be abbreviated *C* and *A*, respectively. It should be noted, however, that Ru(1) and Ru(4) are chiral as well, but, since their chirality is related to the chirality of Ru(2) and Ru(3), respectively, the chirality of Ru(1) and Ru(4) will be omitted in order to avoid the use of redundant chirality descriptors; i.e. *CA* stands for $C_{Ru(2)}A_{Ru(3)}$ and *CC* for $C_{Ru(2)}C_{Ru(3)}$. It should also be noted that upon going from **3** to **5** the *chirality symbols* of the cyclometalated ruthenium atoms change from *A* into *C* and vice versa. (a) Brown, M. F.; Cook, B. R.; Sloan, T. E. *Inorg. Chem.* **1975**, *14*, 1273. (b) Brown, M. F.; Cook, B. R.; Sloan, T. E. *Inorg. Chem.* **1978**, *17*, 1563. (c) Sloan, T. E. In *Topics in Inorganic and Organometallic Stereochemistry*; Geoffroy, G. L., Ed.; Wiley-Interscience: New York, 1981; Vol. 12, p 1. (d) *IUPAC Nomenclature of Inorganic Chemistry, Recommendations 1990*; Blackwell Scientific Publications: Oxford, England, 1990.

reactivity of this new compound[25] are comparable to those of $HRu_2(CO)_5[C_6H_5C{=}C(H)C(H){=}N\text{-}i\text{-}Pr]$ (**2d**), which has previously been isolated and characterized.[6,7] Hence, this species was identified as $HRu_2(CO)_5[CH_3C{=}C(H)C(H){=}N\text{-}i\text{-}Pr]$ (**2a**). During the reactions of **3c** and **3d** with H_2 (1 bar) the intermediacy of **2c** and **2d**, respectively, could be observed as well (IR). After 15 min the concentration of **2a** had reached a steady-state concentration and another reaction was observed. Hydrido complex **2a** slowly converted into (*CC/AA*)-**5a**, $H_4Ru_4(CO)_{12}$, and $CH_3CH_2CH_2CH_2N(H)(i\text{-}Pr)$, as depicted in Scheme I. Furthermore, some $Ru_2(CO)_6[CH_3C{=}C(H)CH_2N\text{-}i\text{-}Pr]$ (**1a**) was formed. No hydride resonances were observed that might be attributed to the other diastereomer, (*CA/AC*)-**5a**. When the reaction was continued at 40 °C, the concentration of (*CA/AC*)-**3a** gradually decreased, whereas the concentration of (*CC/AA*)-**3a** remained unaffected. After about 90 min (*CA/AC*)-**3a** was almost completely converted into (*CC/AA*)-**5a**, $H_4Ru_4(CO)_{12}$, and $CH_3CH_2CH_2CH_2N(H)(i\text{-}Pr)$. Then, the temperature of the sapphire NMR tube was raised stepwise to 70 °C. At this temperature also (*CC/AA*)-**3a** reacted with dihydrogen, whereby the same reaction path as described for (*CA/AC*)-**3a** was followed. After (*CC/AA*)-**3a** was completely hydrogenated as well (after about 30 min at 70 °C), (*CC/AA*)-**5a**, $H_4Ru_4(CO)_{12}$, $CH_3CH_2CH_2CH_2N(H)(i\text{-}Pr)$, and some **1a** were present in the resulting reaction mixture. Throughout this experiment dissolved dihydrogen was present in the deuterated solvent as observed by ^1H NMR spectroscopy ($\delta(H_2)$ C_6D_6, 40 °C: 4.46 ppm).

Dimerization of **2a–d** under an atmosphere of dihydrogen is assumed to produce about equal amounts of (*CA/AC*)-**5a–d** and (*CC/AA*)-**5a–d**. Since only (*CC/AA*)-**5a,b,d** are observed, (*CA/AC*)-**5a–d** and (*CC/AA*)-**5c** are apparently not stable under the applied reaction conditions and are converted into $H_4Ru_4(CO)_{12}$ and hydrogenated MAD at a higher rate than hydrogenation of **3a–d**. A useful advantage of the enhanced reactivity of (*CA/AC*)-**3a** toward H_2 is that it provides a practical chemical method to purify (*CC/AA*)-**3a**. Thus far, purification of (*CC/AA*)-**3a** could only be achieved by preparative HPLC.[4]

Hydrogenation Transfers to the MAD-yl Ligand. The linear tetranuclear clusters $Ru_4(CO)_{10}[R^1C{=}C(H)C(H){=}NR^2]_2$ (R^1, R^2 = CH_3, *i*-Pr (**3a**), CH_3, c-Hex (**3b**), CH_3, *t*-Bu (**3c**), C_6H_5, *i*-Pr (**3d**)) are smoothly converted into the dinuclear compounds $Ru_2(CO)_6[R^1C{=}C(H)CH_2NR^2]$ (**1a–d**; 60–80%) at 90 °C under an atmosphere of H_2/CO (9:1) (eq 2). During this reaction the inner intermetallic bond

$$\underset{\textbf{3a–d}}{Ru_4(CO)_{10}[R^1C{=}C(H)C(H){=}NR^2]_2} + H_2 + 2CO \xrightarrow{90\ °C} 2\underset{\textbf{1a–d}}{Ru_2(CO)_6[R^1C{=}C(H)CH_2NR^2]} \quad (2)$$

$$\underset{\textbf{5a,b,d}}{H_2Ru_4(CO)_8[R^1C{=}C(H)C(H){=}NR^2]_2} + 4CO \xrightarrow{90\ °C} 2\underset{\textbf{1a,b,d}}{Ru_2(CO)_6[R^1C{=}C(H)CH_2NR^2]} \quad (3)$$

in **3** is broken and both of the anionic 7e-donating MAD-yl ligands are regioselectively monohydrogenated to give two dianionic 6e-donating enyl–amido ligands coordinated to $Ru_2(CO)_6$ cores. This reaction constitutes the reverse of the formation of **3**.[6] Interestingly, the formerly inaccessible compound **1c** could also be obtained via this method.[6]

At 90 °C in heptane solution, the 64-electron butterfly clusters $H_2Ru_4(CO)_8[R^1C{=}C(H)C(H){=}NR^2]_2$ (**5a,b,d**) react with CO, also giving **1a,b,d** in nearly quantitative yields (eq 3). During this conversion fragmentation of the tetranuclear clusters into two dinuclear species takes place whereby each dinuclear part takes up two CO ligands. Furthermore, the hydride present in each half of the molecule of **5** is regioselectively transferred to the imine carbon atom of the MAD-yl ligand. A better insight into the course of these reactions was obtained by studying the reaction of $HRu_2(CO)_5[C_6H_5C{=}C(H)C(H){=}N\text{-}i\text{-}Pr]$ (**2d**) with CO. At ambient temperature **2d** rapidly takes up one CO ligand to give $HRu_2(CO)_6[C_6H_5C{=}C(H)C(H){=}N\text{-}i\text{-}Pr]$ (**6d**) (eq 4).

$$\underset{\textbf{2d}}{HRu_2(CO)_5[C_6H_5C{=}C(H)C(H){=}N\text{-}i\text{-}Pr]} + CO \xrightarrow{20\ °C} \underset{\textbf{6d}}{HRu_2(CO)_6[C_6H_5C{=}C(H)C(H){=}N\text{-}i\text{-}Pr]} \quad (4)$$

During this reaction the η^2(C=N)-bonded part of the 7e-donating MAD-yl ligand in **2d** is substituted by a CO ligand. In **6d** the MAD-yl ligand is σ(N)-σ(C)-η^2(C=C) (5e) coordinated. Dinuclear **6d** represents the first ruthenium complex containing a MAD-yl ligand in this specific 5e coordination mode and is isostructural with $HRu_2(CO)_6[C_6H_5C{=}C(H)C(CH_3){=}O]$ and $HOs_2(CO)_6[CH_3CH_2C{=}C(H)C(CH_3){=}O]$, both containing a 5e-donating β-metalated α,β-unsaturated ketone ligand.[26,27] Furthermore, this 5e MAD-yl ligand is reminiscent of the bridging 6e σ(N)-σ(N′)-η^2(C=N) coordination mode of RN=C(H)C(H)=NR (R-DAB) as found in a number of di- and trinuclear transition-metal carbonyl complexes.[28] When a solution of **6d** is heated, this compound smoothly isomerizes into **1d**. This conversion is completed within 5 min in refluxing hexane (bp 68 °C; eq 5).

$$\underset{\textbf{6c,d}}{HRu_2(CO)_6[R^1C{=}C(H)C(H){=}NR^2]} \xrightarrow[\text{c: 80 °C, [CO], 4 h}]{\text{d: 68 °C, 5 min}} \underset{\textbf{1c,d}}{Ru_2(CO)_6[R^1C{=}C(H)CH_2NR^2]} \quad (5)$$

Most likely the thermal reactions of **3** with H_2/CO and of **5** with CO to give **1** proceed via the intermediacy of **2d** and **6d**, as has been outlined in Scheme II.

The complex $HRu_2(CO)_6[CH_3C{=}C(H)C(H){=}N\text{-}t\text{-}Bu]$ (**6c**) could, albeit via another reaction, also be obtained. Conversion of **3c** under an atmosphere of H_2/CO (9:1) at 50 °C gave **6c** in about 50% yield. The reactivity of **6c** differs from that of **6d**. Isomerization of **6c** into **1c** (eq 5) proceeds much slower (4 h at 80 °C in heptane) compared to the isomerization of **6d** and only takes place under an atmosphere of CO. Without CO being present, thermolysis of **6c** gives **3c** as the major product (eq 6).

$$2\underset{\textbf{6c}}{HRu_2(CO)_6[CH_3C{=}C(H)C(H){=}N\text{-}t\text{-}Bu]} \xrightarrow[-H_2,\ -2CO]{80\ °C} \underset{\textbf{3c}}{Ru_4(CO)_{10}[CH_3C{=}C(H)C(H){=}N\text{-}t\text{-}Bu]_2} \quad (6)$$

(24) IR data for this complex (**2a**) were obtained by reacting pure (*CA/AC*)-**3a**[4] with dihydrogen (1 bar) in hexane for 30 min at 40 °C, recording an IR spectrum of the reaction mixture, and correcting for the presence of unreacted (*CA/AC*)-**3a**. The IR data for **2a** thus obtained are included in Table III.

(25) Heating of this complex (**2a**) under nitrogen for a few minutes at 80 °C in heptane solution results in the reverse reaction, yielding parent **3a**. Complex **2a** is air-sensitive; complete decomposition takes place in aerated hexane solution within 30 min.

(26) Domingos, A. J. P.; Johnson, B. F. G.; Lewis, J.; Sheldrick, G. M. *J. Chem. Soc., Chem. Commun.* **1973**, 912.

(27) Arce, A. J.; Boyar, E.; Deeming, A. J. *J. Organomet. Chem.* **1987**, *320*, 385.

(28) van Koten, G.; Vrieze, K. *Adv. Organomet. Chem.* **1982**, *21*, 151.

Scheme I. Hydrogenation of (*CA/AC*)-3a and (*CC/AA*)-3a

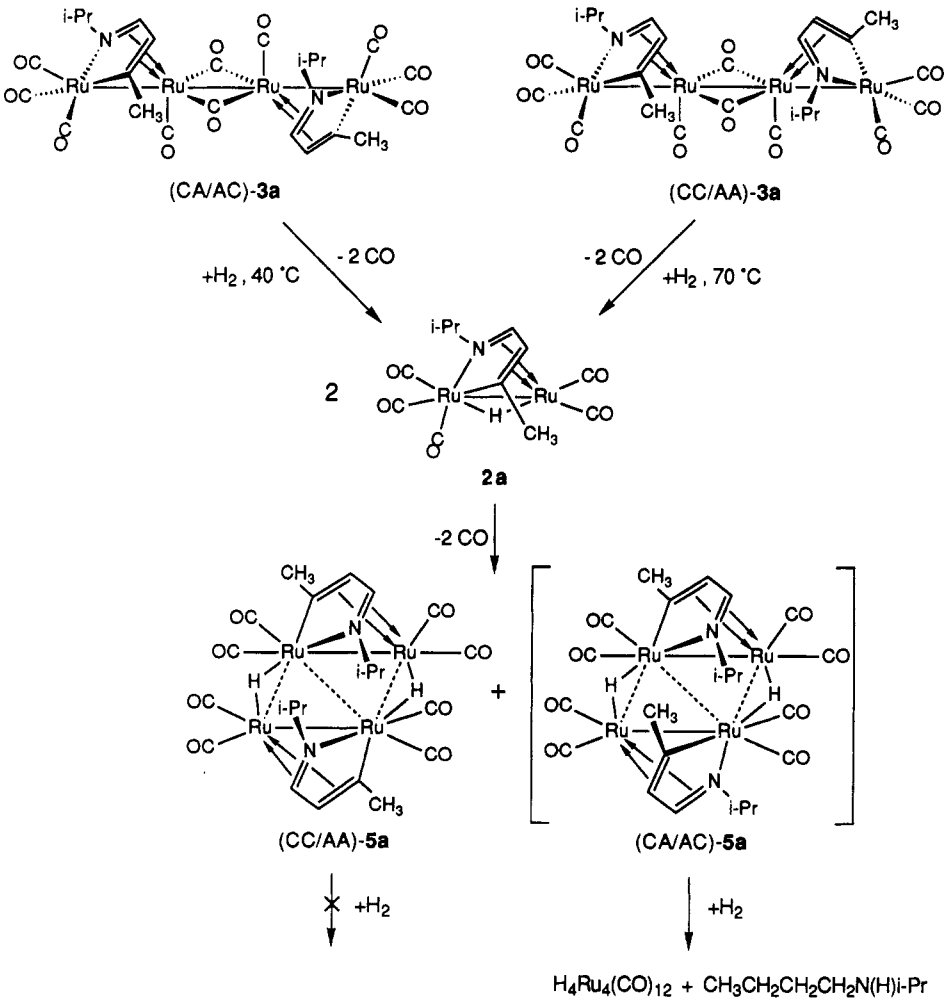

In attempts to isolate the fairly air-resistant dinuclear complexes **6c,d** by column chromatography, it was found that these complexes isomerize on silica into the new complexes $Ru_2(CO)_6[R^1CC(H)C(H)N(H)R^2]$ (**7c,d**) (eq 7).

$$\underset{\textbf{6c,d}}{HRu_2(CO)_6[R^1C{=}C(H)C(H){=}NR^2]} \xrightarrow{[\text{silica}]} \underset{\textbf{7c,d}}{Ru_2(CO)_6[R^1CC(H)C(H)N(H)R^2]} \quad (7)$$

The analogue **7e** (R^1, R^2 = C_6H_5, *t*-Bu) has recently been isolated from the thermal reaction of $Ru_3(CO)_{12}$ with $C_6H_5C(H){=}C(H)C(H){=}N$-*t*-Bu after chromatographic fractionation of the reaction mixture on silica,[6] indicating that **6e** was present in this mixture prior to chromatography. The structures of **7c–e** are based on their IR (showing a ν(NH) stretching mode near 3300 cm^{-1}), ^1H and ^{13}C NMR, and FD-MS characteristics and elemental analyses, which will be discussed. During the formation of this product **7** the hydride as it is present in **6** has, just as during isomerization into **1**, formally migrated to the imine entity of the MAD-yl ligand. In **7**, however, the hydrogen atom is attached to the imine N atom instead of the imine C atom as in **1**. Complex **7** is, just as its parent compound **6**, fairly air-resistant and its formation is irreversible. Therefore, compound **7** cannot be an intermediate in the thermally induced conversion of **6** into **1**. Complex **7d** constitutes the imine-hydrogenated counterpart of $Ru_2(CO)_6[R^1CC(H)C(H)N{=}C(CH_3)_2]$ (**8**).[9] Attempts to dehydrogenate **7d** thermally into $Ru_2(CO)_6[C_6H_5CC(H)C(H)N{=}C(CH_3)_2]$ (**8d**), or, in reverse, to hydrogenate **8a** thermally into **7a**, however, were unsuccessful (Scheme III).

In a previous paper[6] it was proposed that the conversion of **1a–c**, in thermal reactions with MAD or crotonaldehyde, into $Ru_2(CO)_6[CH_2CC(H)C(H){=}NR^2]$ (**4a–c**) proceeded via **6a–c**. In order to examine this hypothesis, **6c** was reacted with an excess of $CH_3C(H){=}C(H)C(H){=}N$-*t*-Bu. It was found that, at 70 °C in heptane solution, **6c** was indeed converted into **4c**. The enhanced thermal stability of **6** and its anomalous decomposition path with R^2 = *t*-Bu (**6c**) compared to the path with R^2 = *i*-Pr (**6d**) also provides a plausible explanation for the findings that neither **1c** nor **1e** is formed during thermal reactions of $Ru_3(CO)_{12}$ with R^1,R^2-MAD, whereas **1d** and **1a,b** are obtained in good yields (50–70%). Apparently, also during the thermal reactions of $Ru_3(CO)_{12}$ with R^1,R^2-MAD, formation of **1** (and **4**) proceeds via the intermediacy of **6**, as outlined in Scheme II.

The compounds $Ru_2(CO)_6[CH_2CC(H)C(H){=}NR^2]$ (R^2 = *i*-Pr (**4a**), *t*-Bu (**4c**)) both react thermally with dihydrogen. The product formation, however, depends on the R^2 substituent. For R^2 = *i*-Pr, a smooth reaction takes place in heptane at 100 °C whereby $Ru_2(CO)_6[CH_3C{=}C(H)CH_2N$-*i*-Pr] (**1a**) is formed in good yield within 0.5 h (eq 8), whereas for R^2 = *t*-Bu conversion of **4** in refluxing heptane proceeds more slowly and gives, surprisingly, $Ru_4(CO)_{10}[CH_3C{=}C(H)C(H){=}N$-*t*-Bu$]_2$ (**3c**) as the main product (eq 9).

$$\underset{\textbf{4a}}{Ru_2(CO)_6[CH_2CC(H)C(H)=N\text{-}i\text{-}Pr]} + H_2 \xrightarrow{100\ ^\circ C} \underset{\textbf{1a}}{Ru_2(CO)_6[CH_3C=C(H)CH_2N\text{-}i\text{-}Pr]} \quad (8)$$

$$2\underset{\textbf{4c}}{Ru_2(CO)_6[CH_2CC(H)C(H)=N\text{-}t\text{-}Bu]} + H_2 \xrightarrow[-2CO]{100\ ^\circ C} \underset{\textbf{3c}}{Ru_4(CO)_{10}[CH_3C=C(H)C(H)=N\text{-}t\text{-}Bu]_2} \quad (9)$$

The product formation of these hydrogenation reactions indicates that they most probably proceed via **6a** and **6c**, respectively. The production of **3c** via this method is useful, since synthesis of **3c** by thermolysis of $Ru_3(CO)_{12}$ and CH_3,*t*-Bu-MAD affords this compound in rather poor yields (≤30%).[6] The stability of **3c** under the reaction conditions applied is very remarkable. As described above, **3c** is thermally unstable under an atmosphere of dihydrogen and decomposes into $H_4Ru_4(CO)_{12}$ and (*n*-Bu)N(H)(*t*-Bu). Apparently, the presence of **4c** during hydrogenation of **3c** prevents decomposition of the latter. This "stabilization" might be caused by a reaction of a hydrogenation product of **3c**, i.e. $HRu_2(CO)_5[CH_3C=C(H)C(H)=N\text{-}t\text{-}Bu]$ (**2c**) or coordinatively unsaturated $HRu_2(CO)_4[CH_3C=C(H)C(H)=N\text{-}t\text{-}Bu]$, with **4c** under re-formation of **3c**. Another possibility is that the presence of small amounts of CO, which are liberated during the conversion of **4c** into **3c**, prevent decomposition of **3c** (Scheme II).

Reaction of $Ru_4(CO)_{10}[CH_3C=C(H)C(H)=N\text{-}i\text{-}Pr]_2$ (3a) with D_2. The reaction of $Ru_4(CO)_{10}[CH_3C=C(H)C(H)=N\text{-}i\text{-}Pr]_2$ (**3a**) with dideuterium at 80 °C in heptane yielded $(H_{0.7}D_{1.3})Ru_4(CO)_8[CH_3C=C(H)C(H_{0.35}D_{0.65})=N\text{-}i\text{-}Pr]_2$ (**5a**), containing approximately 2.6 D atoms per molecule. This indicates the occurrence of H(D)-migration between ruthenium and C_{im} sites. The deuterium atoms were randomly distributed over the imine and the hydride positions, as shown by ^1H NMR spectroscopy. A possible mechanism by which deuterium may be incorporated in the imine position is given in Scheme IV, constituting a reversible reduction of the imine bond in **2a**. The proposed crucial interchange of the σ(C) and η^2(C=C) bonds after transfer of the hydride to the imine C atom has actually been observed for complex **1** by NMR spectroscopy.[6] The thermal reaction of this deuterated **5a** with CO yielded $Ru_2(CO)_6[C(H_{2.8}D_{0.2})C=C(H)C(H_{0.9}D_{1.1})N\text{-}i\text{-}Pr]$ (**1a**). ^2H NMR studies showed not only the presence of about 1.1 D atoms in the "CHD entity" but also a small amount of deuterium in the CH_3 group (0.2 D atom). The (unexpected) incorporation of deuterium at various positions during these reactions shows that, besides the C–H activation and formation processes which have been found to take place on the macroscopic time scale so far (see Scheme II), several similar processes may occur (reversibly) on the microscopic time scale as well in the studied ruthenium carbonyl complexes.[3,4,6,7,9,13,29-31]

Molecular Geometry of (CC/AA)-$(\mu\text{-}H)_2Ru_4(CO)_8[CH_3C=C(H)C(H)=N\text{-}i\text{-}Pr]_2$ ((CC/AA)-5a). The molecular geometry of (*CC/AA*)-**5a**, along with the adopted numbering scheme, is given in Figure 3. In Figure 4 two representative space-filling models of **5a** are shown. Selected bond lengths and bond angles are listed in Tables II and III, respectively. The molecule possesses non-crystallographic C_2 symmetry, with the 2-fold axis running through the midpoints of the $Ru_2\cdots Ru_3$ and $Ru_1\cdots Ru_4$ edges.

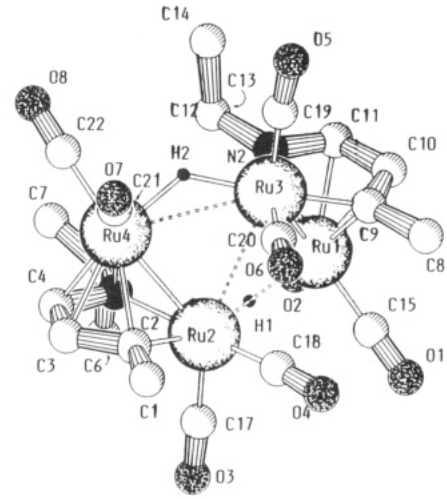

Figure 3. Molecular structure of (*CC/AA*)-**5a**.

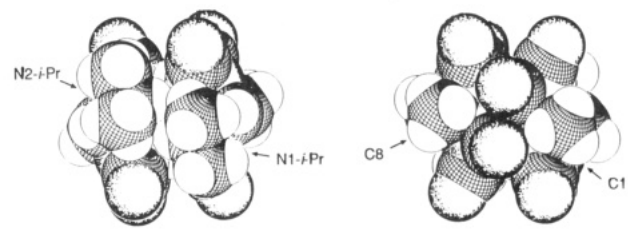

Figure 4. Space-filling models of (*CC/AA*)-**5a**, showing the $(i\text{-Pr})_2$ side (left) and the $(CH_3)_2$ side (right).

Table II. Final Coordinates and Equivalent Isotropic Thermal Parameters and their Esd's in Parentheses for 5a

atom	*x*	*y*	*z*	*U*(eq),[a] Å²
Ru(1)	0.49656 (3)	0.23278 (2)	0.13608 (2)	0.0332 (1)
Ru(2)	0.32246 (3)	0.33405 (2)	0.24140 (2)	0.0293 (1)
Ru(3)	0.54965 (3)	0.23207 (2)	0.31778 (2)	0.0308 (1)
Ru(4)	0.48204 (3)	0.40243 (2)	0.37644 (2)	0.0286 (1)
O(1)	0.2755 (4)	0.1472 (2)	0.0515 (3)	0.086 (2)
O(2)	0.5233 (3)	0.3118 (2)	−0.0373 (2)	0.069 (1)
O(3)	0.1034 (3)	0.3839 (3)	0.1216 (2)	0.082 (2)
O(4)	0.1812 (3)	0.1840 (2)	0.2618 (2)	0.076 (2)
O(5)	0.7437 (3)	0.1679 (2)	0.4490 (2)	0.080 (1)
O(6)	0.3646 (3)	0.1756 (2)	0.4356 (2)	0.080 (2)
O(7)	0.4760 (3)	0.3472 (2)	0.5600 (2)	0.068 (1)
O(8)	0.7218 (3)	0.4921 (2)	0.4232 (2)	0.047 (1)
N(1)	0.4183 (3)	0.4438 (2)	0.2438 (2)	0.034 (1)
N(2)	0.6665 (3)	0.2624 (2)	0.2217 (2)	0.039 (1)
C(1)	0.1855 (4)	0.3506 (3)	0.4113 (3)	0.052 (2)
C(2)	0.2728 (3)	0.3861 (2)	0.3511 (2)	0.037 (1)
C(3)	0.3014 (4)	0.4667 (2)	0.3607 (3)	0.042 (1)
C(4)	0.3806 (4)	0.4976 (2)	0.3029 (3)	0.040 (1)
C(5)	0.4862 (4)	0.4752 (2)	0.1720 (3)	0.044 (1)
C(6)	0.3922 (5)	0.5034 (3)	0.0995 (3)	0.063 (2)
C(7)	0.5819 (5)	0.5379 (3)	0.1981 (3)	0.063 (2)
C(8)	0.4618 (5)	0.0616 (3)	0.2533 (4)	0.070 (2)
C(9)	0.5348 (4)	0.1355 (3)	0.2401 (3)	0.046 (2)
C(10)	0.6216 (4)	0.1310 (3)	0.1789 (3)	0.056 (2)
C(11)	0.6923 (4)	0.2010 (3)	0.1680 (3)	0.052 (2)
C(12)	0.7457 (4)	0.3344 (3)	0.2226 (3)	0.054 (2)
C(13)	0.7833 (5)	0.3631 (4)	0.1350 (3)	0.077 (2)
C(14)	0.8573 (5)	0.3212 (4)	0.2873 (4)	0.085 (2)
C(15)	0.3587 (4)	0.1801 (3)	0.0832 (3)	0.053 (2)
C(16)	0.5157 (4)	0.2844 (3)	0.0276 (3)	0.047 (2)
C(17)	0.1889 (4)	0.3638 (3)	0.1652 (3)	0.047 (2)
C(18)	0.2399 (4)	0.2399 (3)	0.2553 (3)	0.046 (1)
C(19)	0.6688 (4)	0.1958 (3)	0.4007 (3)	0.048 (2)
C(20)	0.4319 (4)	0.1985 (3)	0.3898 (3)	0.047 (2)
C(21)	0.4830 (4)	0.3684 (3)	0.4904 (3)	0.045 (1)
C(22)	0.6332 (4)	0.4599 (3)	0.4047 (3)	0.046 (1)

[a] U_{eq} is equal to one-third of the orthogonalized **U** matrix.

(29) Mul, W. P.; Elsevier, C. J.; Spaans, J. *J. Organomet. Chem.* **1991**, *402*, 125.

(30) (a) Mul, W. P.; Elsevier, C. J.; Vrieze, K.; Smeets, W. J. J.; Spek, A. L. *Recl. Trav. Chim. Pays-Bas* **1988**, *107*, 297. (b) Mul, W. P.; Elsevier, C. J.; Smeets, W. J. J.; Spek, A. L. *Inorg. Chem.* **1991**, *30*, 4152.

(31) Beers, O. C. P.; Elsevier, C. J.; Mul, W. P.; Vrieze, K.; Häming, L. P.; Stam, C. H. *Inorg. Chim. Acta* **1990**, *171*, 129.

Scheme II. Hydrogenation, Dehydrogenation, and H-Transfer Reactions in the $Ru_3(CO)_{12}/R^1,R^2$-MAD System[c]

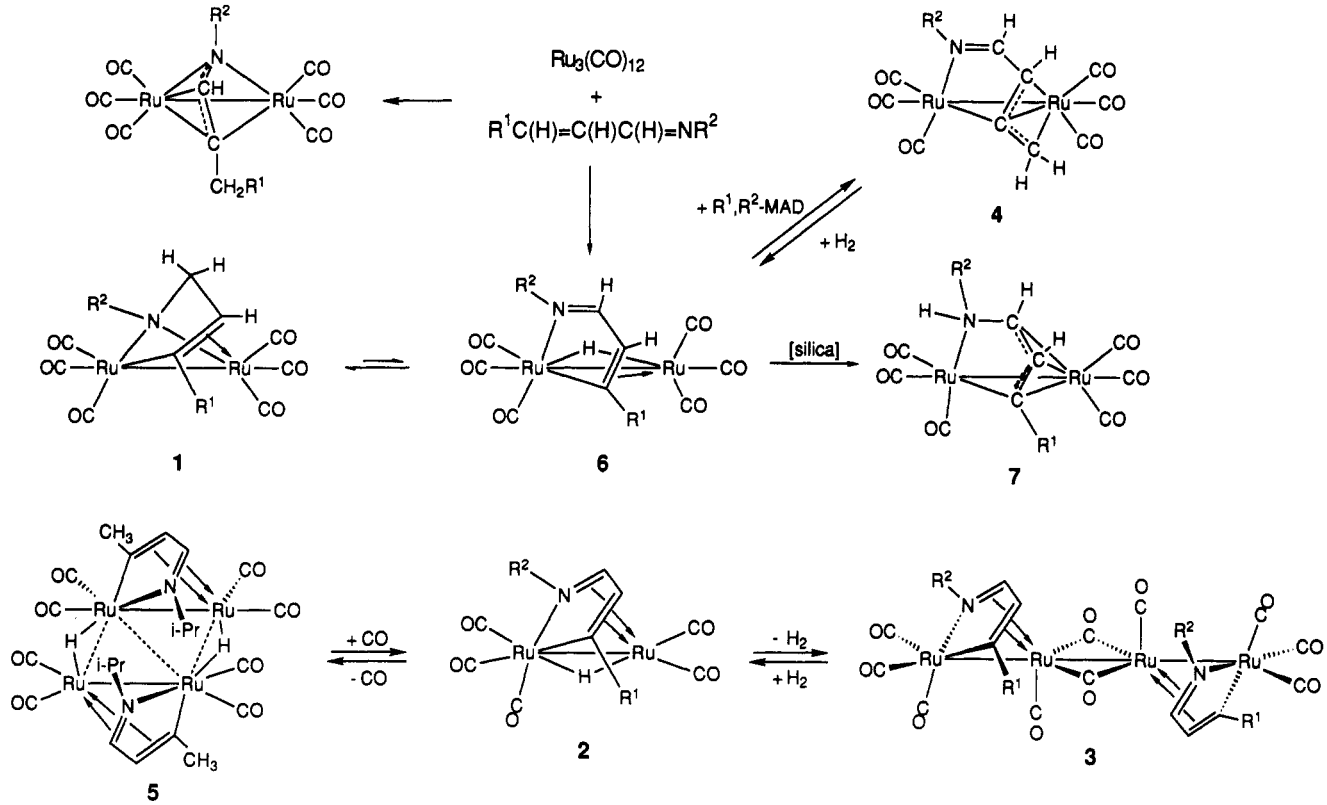

[c] Legend: R^1, R^2 = CH_3, *i*-Pr (**a**); CH_3, c-Hex (**b**); CH_3, *t*-Bu (**c**); C_6H_5, *i*-Pr (**d**); C_6H_5, *t*-Bu (**e**).

Scheme III. Attempted Hydrogenation/Dehydrogenation Reactions

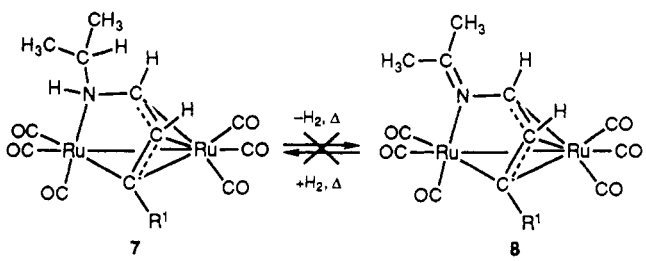

The present tetranuclear ruthenium cluster is an aggregate of two $Ru_2(CO)_4[CH_3C{=}C(H)\text{-}C(H){=}N\text{-}i\text{-}Pr]$ units and two bridging hydrides. The four ruthenium atoms occupy a butterfly arrangement and are mutually connected by two bonds of normal length (Ru(1)–Ru(3) = 2.8144 (6) Å and Ru(2)–Ru(4) = 2.8262 (6) Å) and three long bonds (Ru(1)–Ru(2) = 3.1230 (6) Å, Ru(2)–Ru(3) = 3.1409 (6) Å, and Ru(3)–Ru(4) = 3.1243 (6) Å), while there is no bonding interaction between Ru(1) and Ru(4), the intermetallic Ru(1)···Ru(4) distance being 4.7091 (8) Å. The dihedral angle ϕ between the two triangular units Ru(1)Ru(2)Ru(3) and Ru(2)Ru(3)Ru(4) amounts to 137.05°, which is indicative of a flattened butterfly.[32]

The Ru(1)–Ru(3) and Ru(2)–Ru(4) bonds are both bridged by a 7e-donating *N*-isopropylcrotonaldimin-4-yl ligand (CH_3,*i*-Pr-MAD-yl) and are ca. 0.11 Å longer than the relevant intermetallic bonds in (*CC/AA*)-$Ru_4(CO)_{10}[CH_3C{=}C(H)C(H){=}N\text{-}i\text{-}Pr]_2$ (**3a**)[3] and (*CC/AA*)-$Ru_3(CO)_6[CH_3C{=}C(H)C(H){=}N\text{-}i\text{-}Pr]_2$ (**9a**).[30]

Most likely, the hydrides bridge the Ru(1)–Ru(2) and Ru(3)–Ru(4) edges, as indicated by their restrained refinement (hampered by the minor disorder peaks of the Ru_4 core). Bridging hydrides (μ_2-H) generally cause an increase of the bridged Ru–Ru bond by 0.15–0.20 Å.[33] Taking the average Ru–Ru distance in $Ru_3(CO)_{12}$, which amounts to 2.854 (4) Å (mean),[34] as the starting point, one ends up with an expected bond length of 3.00–3.05 Å for a ruthenium–ruthenium bond bridged by a hydride. The observed hydride-bridged Ru(1)–Ru(2) and Ru(3)–Ru(4) bonds in **5a**, however, are even longer by ca. 0.10 Å.

The butterfly configuration is usually associated with a 62-electron count, and since **5a** contains 64 closed valence electrons (CVE),[35] this cluster represents an electron-rich member of this geometrical class. From the bonding characteristics discussed above, it is apparent that in **5a** the two additional electrons are placed in an orbital which possesses significant metal–metal antibonding character. This antibonding orbital is probably delocalized over all four ruthenium atoms, since the four outer Ru–Ru bonds are lengthened, and also the hinge bond (Ru(2)–Ru(3)) is long. In several other 64e tetranuclear metal carbonyl clusters as well, flattened butterfly arrangements have been observed with weakened M–M bonds.[32,36]

Cluster **5a** contains eight terminally bonded CO ligands which exhibit normal geometric features and two MAD-yl

(32) Carty, A. J.; MacLaughlin, S. A.; van Wagner, J.; Taylor, N. J. *Organometallics* **1982**, *1*, 1013.

(33) Bennett, M. A.; Bruce, M. I.; Matheson, T. W. In *Comprehensive Organometallic Chemistry*; Wilkinson, G., Stone, F. G. A., Abel, E. W., Eds.; Pergamon: Oxford, England, 1982; Vol. 4, p 846.

(34) Churchill, M. R.; Hollander, F. J.; Hutchinson, J. P. *Inorg. Chem.* **1977**, *16*, 2655.

(35) (a) Lauher, J. W. *J. Am. Chem. Soc.* **1978**, *100*, 5305. (b) Lauher, J. W. *J. Organomet. Chem.* **1981**, *213*, 25.

(36) (a) Staal, L. H.; Polm, L. H.; Vrieze, K.; Ploeger, F.; Stam, C. H. *Inorg. Chem.* **1981**, *20*, 3590. (b) Churchill, M. R.; Bueno, C.; Young, D. A. *J. Organomet. Chem.* **1981**, *213*, 139. (c) Carty, A. J.; MacLaughlin, S. A.; van Wagner, J.; Taylor, N. J. *Organometallics* **1982**, *1*, 1013. (d) Adams, R. D.; Yang, L. W. *J. Am. Chem. Soc.* **1983**, *105*, 235. (e) Hogarth, G.; Phillips, J. A.; van Gastel, F.; Taylor, N. J.; Marder, T. B.; Carty, A. J. *J. Chem. Soc., Chem. Commun.* **1988**, 1570.

Scheme IV. Proposed Mechanism for the Incorporation of Deuterium on C_{im} in the Intermediate 2a during the Conversion of 3a into 5a

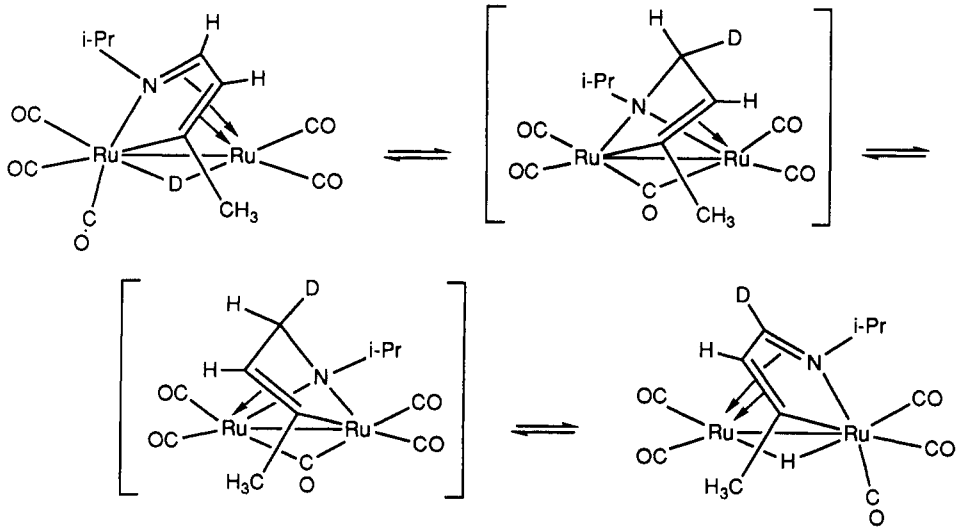

Table III. Selected Bond Distances (Å) and Bond Angles (deg) for 5a

Ru(1)-Ru(2)	3.1230 (6)	Ru(1)-H(1)	1.60 (5)	Ru(4)-C(3)	2.233 (4)
Ru(1)-Ru(3)	2.8144 (6)	Ru(2)-C(2)	2.031 (3)	Ru(4)-C(4)	2.200 (4)
Ru(2)-Cu(3)	3.1409 (6)	Ru(2)-C(17)	1.846 (5)	Ru(4)-C(21)	1.854 (5)
Ru(2)-Ru(4)	2.8262 (6)	Ru(2)-C(18)	1.847 (5)	Ru(4)-C(22)	1.919 (5)
Ru(3)-Ru(4)	3.1243 (6)	Ru(2)-N(1)	2.123 (3)	Ru(4)-N(1)	2.214 (3)
Ru(1)···Ru(4)	4.7091 (8)	Ru(2)-H(1)	1.83 (5)	Ru(4)-H(2)	1.74 (3)
Ru(1)-C(9)	2.308 (5)	Ru(3)-C(9)	2.022 (5)	C(2)-C(3)	1.400 (5)
Ru(1)-C(10)	2.248 (5)	Ru(3)-C(19)	1.835 (5)	C(3)-C(4)	1.401 (6)
Ru(1)-C(11)	2.199 (4)	Ru(3)-C(20)	1.864 (5)	N(1)-C(4)	1.379 (5)
Ru(1)-C(15)	1.860 (5)	Ru(3)-N(2)	2.110 (3)	C(9)-C(10)	1.402 (6)
Ru(1)-C(16)	1.921 (5)	Ru(3)-H(2)	1.72 (3)	C(10)-C(11)	1.428 (7)
Ru(1)-N(2)	2.220 (3)	Ru(4)-C(2)	2.283 (3)	N(2)-C(11)	1.374 (6)

Ru(2)-Ru(1)-Ru(3)	63.63 (1)	Ru(2)-Ru(4)-C(22)	145.4 (1)
Ru(3)-Ru(1)-C(15)	121.0 (1)	Ru(2)-Ru(4)-Ru(3)	63.49 (1)
Ru(3)-Ru(1)-C(16)	147.8 (2)	Ru(2)-Ru(4)-C(21)	121.5 (2)
Ru(1)-Ru(2)-Ru(3)	53.40 (1)	Ru(1)-H(1)-Ru(2)	131 (3)
Ru(1)-Ru(2)-Ru(4)	104.55 (2)	Ru(3)-H(2)-Ru(4)	129 (2)
Ru(3)-Ru(2)-Ru(4)	62.88 (1)	C(4)-N(1)-C(5)	117.5 (3)
Ru(4)-Ru(2)-C(2)	53.05 (9)	C(11)-N(2)-C(12)	118.0 (3)
Ru(4)-Ru(2)-C(17)	138.3 (2)	C(1)-C(2)-C(3)	117.7 (3)
Ru(4)-Ru(2)-C(18)	122.3 (1)	C(2)-C(3)-C(4)	115.9 (4)
Ru(4)-Ru(2)-N(1)	50.74 (8)	C(3)-C(4)-N(1)	114.8 (3)
N(1)-Ru(2)-C(2)	77.2 (1)	C(8)-C(9)-C(10)	116.4 (4)
N(1)-Ru(2)-C(18)	172.3 (2)	C(9)-C(10)-C(11)	116.1 (4)
Ru(1)-Ru(3)-Ru(2)	62.97 (1)	C(10)-C(11)-N(2)	114.1 (4)
Ru(1)-Ru(3)-Ru(4)	104.81 (2)	Ru(1)-C(15)-O(1)	179.1 (4)
Ru(2)-Ru(3)-Ru(4)	53.63 (1)	Ru(1)-C(16)-O(2)	176.8 (4)
Ru(1)-Ru(3)-C(9)	54.0 (1)	Ru(2)-C(17)-O(3)	176.4 (4)
Ru(1)-Ru(3)-C(19)	139.6 (2)	Ru(2)-C(18)-O(4)	175.3 (4)
Ru(1)-Ru(3)-C(20)	120.9 (1)	Ru(3)-C(19)-O(5)	174.8 (4)
N(2)-Ru(3)-C(9)	78.2 (2)	Ru(3)-C(20)-O(6)	176.6 (4)
N(2)-Ru(3)-C(20)	171.8 (2)	Ru(4)-C(21)-O(7)	175.9 (4)
Ru(1)-Ru(3)-N(2)	51.17 (9)	Ru(4)-C(22)-O(8)	178.0 (4)

ligands which adopt a bridging σ(C)-σ(N)-η^2(C=C):η^2-(C=N) coordination mode and each donate 7e to the cluster core, just as in **2**, **3**, and **9**.[3,4,7,30] The internuclear distances and angles within the MAD-yl ligands are comparable to those found in the crystal structures of **2d**,[7] (*CA/AC*)-**3a**,[3] (*CC/AA*)-**3a**,[4] (*CA/AC*)-**9a**, and (*CC/AA*)-**9a**,[30] indicating extensive electron delocalization within the C=C—C=N skeletons. The distances of the Ru(1) and Ru(4) atoms to the unsaturated C=C—C=N moieties are intermediate between those observed in (*CC/AA*)- and (*CA/AC*)-**3a** and in (*CA/AC*)- and (*CC/AA*)-**9a** and are roughly comparable to those found in **2d**. As discussed before,[7] these distances are believed to be a reflection of the π-back-donating properties of the π-coordinated ruthenium centers (in **5a**: Ru(1) and Ru(4)), properties directly related to the basicity of these metal atoms. The electron density on Ru(1) and Ru(4) in **5a** thus seems to be intermediate between those of the relevant ruthenium centers in **3a** and **9a** and similar to that of **2d**. This is best explained by considering the number of CO ligands that are attached to these ruthenium atoms: in **3a** two bridging and one terminal CO ligands,[3,4] in **2d**[7] and **5a** two terminal CO ligands, and not one CO ligand in **9a**.[30] Since bridging CO ligands are better π-acceptors than terminal CO ligands, the electron-withdrawing capacity of the CO ligands decreases in the series **3a** > **2d** ≈ **5a** > **9a**. The electron density on the ruthenium atoms that are π-coordinated by a MAD-yl ligand is therefore considered to be the reverse of this series. Hence, the shortening of the Ru–MAD-yl distances observed on going from **3a** to **9a** harmonizes with the higher electron density of the ruthenium atoms in this series.

Table IV. IR Data for $Ru_2(CO)_6[CH_3C{=}C(H)CH_2N\text{-}t\text{-}Bu]$ (1c), $HRu_2(CO)_5[CH_3C{=}C(H)C(H){=}NR^2]$ (R^2 = *i*-Pr (2a), *t*-Bu (2c)), $H_2Ru_4(CO)_8[R^1C{=}C(H)C(H){=}NR^2]_2$ (R^1, R^2 = CH_3, *i*-Pr (5a), CH_3, c-Hex (5b), C_6H_5, *i*-Pr (5d)), $HRu_2(CO)_6[R^1C{=}C(H)C(H){=}NR^2]$ (R^1, R^2 = CH_3, *t*-Bu (6c), C_6H_5, *i*-Pr (6d)), and $Ru_2(CO)_6[R^1CC(H)C(H)N(H)R^2]$ (R^1, R^2 = CH_3, *t*-Bu (7c), C_6H_5, *i*-Pr (7d), C_6H_5, *t*-Bu (7e))

compd	solv	ν(CO), cm^{-1}					
1c	*a*	2075 (m)	2046 (s)	1996 (vs)	1986 (m)	1980 (m)	
2a	*a*	2070 (m)	2015 (m)	2004 (s)	1944 (m)		
2c	*a*	2082 (m)	2004 (vs)	1992 (s)	1942 (m)		
5a	*a*	2019 (vs)	2003 (m)	1997 (m)	1972 (s)	1938 (m)	
5b	*a*	2019 (vs)	2003 (m)	1996 (m)	1972 (s)	1938 (m)	
5d	*b*	2020 (vs)	2004 (m)	1997 (sh)	1969 (m)	1933 (m)	
6c	*a*	2089 (m)	2047 (vs)	2018 (s)	1995 (w)	1988 (s)	1969 (m)
6d	*a*	2093 (m)	2054 (s)	2024 (m)	2019 (m)	1996 (m)	1974 (m)
7c[c]	*a*	2070 (m)	2032 (vs)	1997 (vs)	1983 (s)	1974 (m)	1965 (w)
7d[d]	*a*	2074 (m)	2037 (vs)	2003 (s)	1986 (m)	1980 (m)	1967 (w)
7e	*a*	2073 (m)	2037 (s)	2003 (s)	1986 (m)	1979 (m)	1967 (w)

[a] Hexane. [b] Dichloromethane. [c] ν(NH) = 3302 cm^{-1} (KBr pellet). [d] ν(NH) = 3282 cm^{-1} (KBr pellet).

Table V. ^1H NMR Data for $Ru_2(CO)_6[CH_3C{=}C(H)CH_2N\text{-}t\text{-}Bu]$ (1c) $HRu_2(CO)_5[CH_3C{=}C(H)C(H){=}N\text{-}i\text{-}Pr]$[1] (2a) $H_2Ru_4(CO)_8[R^1C{=}C(H)C(H){=}NR^2]_2$ (R^1, R^2 = CH_3, *i*-Pr (5a), CH_3, c-Hex (5b), C_6H_5, *i*-Pr (5d)), $HRu_2(CO)_6[R^1C{=}C(H)C(H){=}NR^2]$ (R^1, R^2 = CH_3, *t*-Bu (6c), C_6H_5, *i*-Pr (6d)), and $Ru_2(CO)_6[R^1CC(H)C(H)N(H)R^2]$ (R^1, R^2 = CH_3, *t*-Bu (7c), C_6H_5, *i*-Pr (7d), C_6H_5, *t*-Bu (7e))[a]

compd	δ, ppm
1c[b]	4.87 (s, C=C*H*); 3.96 (br s, NCH_2); 2.54 (s, C=CCH_3); 1.01 (s, C(CH_3)$_3$)
1c[c]	4.83 (s, C=C*H*); 4.02 (dd, 9.0, 2.4, NC*H*H); 3.82 (d, 9.0, NCH*H*); 2.50 (s, C=CCH_3); 0.95 (s, C(CH_3)$_3$)
2a[d]	6.12 (br s, N=C*H*); 5.45 (br s, C=C*H*); 2.01 (s, C=CCH_3); 0.62/0.57 (d, 6.5, NCH(CH_3)$_2$); -9.77 (s, hydr)
5a[e]	6.91 (d, 2.1, N=C*H*); 5.52 (d, 2.1, C=C*H*); 2.80 (sept, 6.5, NC*H*(CH_3)$_2$); 2.74 (s, C=CCH_3); 1.44/0.97 (d, 6.5, NCH(CH_3)$_2$); -11.94 (s, hydr)
5b[e]	6.95 (d, 2.1, N=C*H*); 5.44 (d, 2.1, C=C*H*); 2.75 (s, C=CCH_3); 1.8-1.2 (br m, NC$_6H_{11}$); -12.10 (s, hydr)
5d	7.35-7.14 (m, C$_6H_5$); 7.01 (d, 2.0, N=C*H*); 5.74 (d, 2.0, C=C*H*); 2.84 (sept, 6.5, NC*H*(CH_3)$_2$); 1.51/1.04 (d, 6.5, NCH(CH_3)$_2$); -12.69 (s, hydr)
6c	7.85 (d, 2.5, N=C*H*); 3.24 (s, C=CCH_3); 2.86 (d, 2.5, C=C*H*); 1.10 (s, C(CH_3)$_3$); -13.10 (s, hydr)
6d	8.02 (d, 2.5, N=C*H*); 7.63-7.12 (m, C$_6H_5$); 3.30 (sept, 6.5, NC*H*(CH_3)$_2$); 2.94 (d, 2.5, C=C*H*); 1.08, 1.03 (d, 6.5, NCH(CH_3)$_2$); -13.06 (s, hydr)
7c	5.62 (d, 2.5, CH_3CC*H*); 4.31 (dd, 2.5, 1.6, C*H*N); 2.88 (d, 0.5, CH_3CH); 2.79 (br s, N(*H*)); 0.96 (s, C(CH_3)$_3$)
7d	7.60-7.15 (m, C$_6H_5$); 5.87 (d, 2.7, CH$_3$CC*H*); 4.24 (dd, 2.7, 1.5, C*H*N); 2.57 (br s, N(*H*)); 2.26 (sept, 6.5, NC*H*(CH$_3$)$_2$); 1.02, 0.98 (d, 6.5, NCH(CH_3)$_2$)
7e	7.60-7.30 (m, C$_6H_5$); 5.87 (d, 2.5, CH$_3$CC*H*); 4.28 (dd, 2.5, 1.5, C*H*N); 2.82 (br s, N(*H*)); 1.00 (s, C(CH_3)$_3$)

[a] Measured in $CDCl_3$, 100 MHz, at room temperature unless stated otherwise. Multiplicities, *J* values (in Hz), and assignments are given in parentheses. [b] 318 K. [c] 263 K. [d] C_6D_6. [e] CD_2Cl_2.

An interesting feature of **5a** is the mutual cis arrangement of the two N-*i*-Pr groups, which are both placed in the cavity between the wingtips of the cluster. The spheres of the two *i*-Pr groups leave little space in this hole, as can be inferred from some intramolecular intersubstituent distances (H(121)-H(51) = 2.271 (6) Å, H(121)-C(5) = 2.900 (6) Å, and H(51)-C(12) = 2.930 (6) Å) and the space-filling model shown on the left-hand side of Figure 4. These distances provide a likely explanation for the fact that formation of **5c** is not observed. Substitution of the two *i*-Pr groups in **5a** by two sterically more demanding *t*-Bu groups, affording $H_2Ru_4(CO)_8[CH_3C{=}C(H)C(H){=}N\text{-}t\text{-}Bu]_2$ (**5c**), will result in a considerable mutual steric interaction of the bulky *t*-Bu groups and destabilize the cluster. Hence, further hydrogenation reactions of **5c** are easy to conceive.

Due to the presence of two intrinsically asymmetric MAD-yl ligands one might expect **5a** to be formed in two diastereomers,[22] which are shown in Figure 2. In the course of the formation of **5a**, only the *CC/AA* enantiomeric pair has been formed, of which the *AA* enantiomer[23] is depicted in Figure 3. Since the space group is $P2_1/n$, the *CC* enantiomer is also present in the unit cell. The second, unobserved *CA/AC* enantiomeric pair of **5a** would contain one N-*i*-Pr group and one CH_3 group in adjacent positions, as shown in Figure 2. The reason it is not observed will be discussed later on.

Spectroscopic Properties of $H_2Ru_4(CO)_8[R^1C{=}C(H)C(H){=}NR^2]_2$ (5). The IR, ^1H NMR, and ^{13}C NMR data for the new tetranuclear dihydrido clusters **5a,b,d** are given in Tables IV-VI, respectively.

The presence of similar five-band IR patterns for **5a,b,d** in hexane or dichloromethane solution in the terminal ν(CO) region (1930-2030 cm^{-1}) indicates that these octacarbonyl complexes are isostructural. FI/FD-MS spectra of **5a,b,d** showed molecular ion patterns at values corresponding to the masses of the isotopes of $H_2Ru_4(CO)_8[R^1C{=}C(H)C(H){=}NR^2]_2$ (see Experimental Section).

The NMR data for **5a** in solution are consistent with the molecular structure in the solid state. Due to C_2 symmetry in the complex the $\{HRu_2(CO)_4[CH_3C{=}C(H)C(H){=}N\text{-}i\text{-}Pr]\}$ halves are equivalent. Consequently, in **5a** both MAD-yl ligands and both hydrides appear as one set of resonances. In CD_2Cl_2 the imine proton H_{im} appears as a doublet at 6.91 ppm (^3J = 2.1 Hz) due to coupling with the olefin proton H_α, which is found at 5.44 ppm.[5] These δ values are within the regions of 6.2-7.5 ppm for H_{im} and 5.0-5.7 ppm for H_α, usually observed for 7e-bonded MAD-yl ligands in $CDCl_3$ or CD_2Cl_2 solution.[3,4,6,30] We note, however, that these chemical shifts are markedly dependent on the solvent, as has been documented for **3a**.[4] The diastereotopic *i*-Pr methyl groups appear as two doublets at 1.44 and 0.97 ppm, whereas the corresponding *i*-Pr CH protons are found as a septet at 2.80 ppm. The methyl H_γ protons[5] are found as a singlet at 2.74 ppm, the δ value being slightly higher when compared to those observed for the *CA/AC* and *CC/AA* diastereomers of **3a**.[3,4,6] The chemical shift of the bridging hydrides of **5a** is found at -11.94 ppm, which is within the expected range.[37] The

(37) Bridging hydrides in ruthenium carbonyl complexes are usually observed between -10 and -30 ppm in ^1H NMR spectra.

Table VI. ^{13}C NMR Data for $Ru_2(CO)_6[CH_3C{=}C(H)CH_2N\text{-}t\text{-}Bu]$ (1c), $H_2Ru_4(CO)_8[CH_3C{=}C(H)C(H){=}N\text{-}i\text{-}Pr]_2$ (5a), $HRu_2(CO)_6[R^1C{=}C(H)C(H){=}NR^2]$ (R^1, R^2 = CH_3, t-Bu (6c), C_6H_5, i-Pr (6d)), and $Ru_2(CO)_6[R^1CC(H)C(H)N(H)R^2]$ (R^1, R^2 = CH_3, t-Bu (7c), C_6H_5, i-Pr (7d), C_6H_5, t-Bu (7e))[a]

compd	δ, ppm
1c[b]	200.0. 198.4, 197.0, 196.6, 194.9, 194.3 (6 × CO), 187.8 (CH_3C=CH), 76.5 (C=CH), 68.0 ($CHCH_2N$), 59.5 ($NC(CH_3)_3$), 35.1 (CH_3C=CH), 31.2 ($NC(CH_3)_3$)
5a[c]	203.0, 200.7, 199.4, 198.4 (4 × CO),[d] 195.8 (CH_3C=CH), 111.5 (HC=N), 92.2 (C=CH), 59.5 ($NCH(CH_3)_2$), 33.7 (CH_3C=CH), 28.9, 20.7 (2 × $NCH(CH_3)_2$)
6c[e]	193.7, 193.4, 190.9 (3 × CO), 151.4 (CH_3C=CH), 175.7 (HC=N), 53.4 (C=CH), 58.3 ($NC(CH_3)_3$), 35.6 (CH_3C=CH), 29.0 ($NC(CH_3)_3$)
6d[c]	194.2, 193.8, 192.3 (3 × CO), 180.6 (HC=N), 154.1/150.3 (C_6H_5C=CH/C_i), 129.9, 128.4, 125.8 (C_6H_5), 60.7 ($NCH(CH_3)_2$), 48.6 (C=CH), 22.7, 21.9 (2 × $NCH(CH_3)_2$)
7c[b]	200.9, 199.6, 193.9 (3 × CO), 170.5 (C=CCH_3), 89.5 (CCHCH), 57.2 (CHCHN), 57.8 ($NC(CH_3)_3$), 31.9 (CH_3C=CH), 27.1 ($NC(CH_3)_3$)
7d[e]	199.7, 198.3, 192.0 (3 × CO), 169.9 (C=CCH_3) 148.2 (C_i), 128.3, 127.6, 126.6 (C_6H_5), 89.5 (CCHCH), 59.7/58.6 ($NCH(CH_3)_2$/CHCHN), 20.1 (2 × $NCH(CH_3)_2$)
7e[b]	205.1, 200.5 (2 × CO), 170.3 (C=CCH_3), 149.1 (C_i), 129.0, 128.4, 127.3 (C_6H_5), 91.7 (CCHCH), 58.2 ($NC(CH_3)_3$), 56.7 (CHCHN), 27.2 ($NC(CH_3)_3$)

[a] Measured at 263 K. [b] $CDCl_3$, 25.0 MHz. [c] CD_2Cl_2, 62.9 MHz. [d] Deduced from a ^{13}CO-enriched sample. [e] $CDCl_3$, 62.9 MHz.

^1H NMR resonances of **5b** and **5d** are comparable with those of **5a**, although the hydrides resonate at somewhat different δ values (**5b**, −12.10 ppm; **5d**, −12.69 ppm).

Both purified samples and crude reaction mixtures of **5a,b,d** show only one set of ^1H NMR signals, indicating the presence of only one diastereomer for all compounds. If both diastereomers were present, a double set of resonances would be expected in the NMR spectra of **5a,b,d**, similar to the spectra observed for diastereomeric mixtures of (*CA/AC*)- and (*CC/AA*)-**3a** and (*CA/AC*)- and (*CC/AA*)-$Ru_3(CO)_6[CH_3C{=}C(H)C(H){=}N\text{-}i\text{-}Pr]_2$ (**9a**).[4,30]

The ^{13}C NMR spectrum of **5a** recorded in CD_2Cl_2 at 263 K shows one set of resonances for the two equivalent *N*-isopropylcrotonaldimin-4-yl ligands and four resonances corresponding to the eight CO ligands. Discrimination between the five resonances observed in the region of 195–203 ppm was achieved by recording a ^{13}C NMR spectrum of a ^{13}CO-enriched sample of **5a**, which was prepared from ^{13}CO-enriched **3a**.[4] Four CO signals are observed as sharp singlets at 203.0, 200.7, 199.4, and 198.4 ppm, indicating that the CO ligands of **5a** are not fluxional, which is remarkable for a tetranuclear carbonyl cluster of the iron triad. Probably the rigid MAD-yl ligands and the hydrides hamper facile CO exchange processes in **5a**. The fifth signal present in the "CO region" at 195.8 ppm is attributable to the metalated C_β atoms and is found at a δ value very similar to those found for the two diastereomers of **3a**.[4] This chemical shift is about 64 ppm higher compared to the free ligand value of 131.7 ppm,[3] which is best ascribed to a certain degree of π-bonding between Ru(2) and C_β (and Ru(3) and C'_β) causing an increased paramagnetic contribution to the shielding of C_β.

The imine and olefin carbon atoms C_{im} and C_α of **5a** are observed at 111.5 and 92.2 ppm, respectively, δ values notably lower than those found for the two diastereomers of **3a** ($C_{im} \approx 130$ ppm, $C_\alpha \approx 104$ ppm).[3,4] The lower δ values found for **5a** point to a stronger π back-donation from the relevant Ru(1) and Ru(4) d orbitals into the π* orbitals of the C=C—C=N entities, thus causing a less pronounced paramagnetic deshielding of the C_{im} and C_α atoms in **5a** compared to that in **3a**. The stronger bonding of the π system of the MAD-yl ligand to the cluster core in **5a** compared to that in both diastereomers of **3a** could also be inferred from the Ru–π-C=C and Ru–π-C=N distances, as found in their crystal structures (vide infra).

Spectroscopic Properties of the Dinuclear Complexes. IR: ν(CO) and ν(NH) Region. The new dinuclear complexes reported in this paper show characteristic patterns in the ν(CO) region (see Table IV). Four ($HRu_2(CO)_5[CH_3C{=}C(H)C(H){=}NR^2]$ (**2a,c**)), five ($Ru_2(CO)_6[CH_3C{=}C(H)CH_2N\text{-}t\text{-}Bu]$ (**1c**)), or six ($HRu_2(CO)_6[R^1C{=}C(H)C(H){=}NR^2]$ (**6c,d**), $Ru_2(CO)_6[R^1CC(H)C(H)N(H)R^2]$ (**7c–e**)) IR bands are observed in the terminal region of 1930–2100 cm^{-1}. The IR spectra of **1c** and **2a,c** roughly parallel those of the formerly reported complexes **1a,b,d** and **2d**, respectively, of which **1a** and **2d** have been characterized by crystal structures.[3,7] The IR spectra of the complexes $Ru_2(CO)_6[CH_3CC(H)C(H)N(H)R^2]$ (**7**) are very much like those of $Ru_2(CO)_6[CH_3CC(H)C(H)N{=}C(CH_3)_2]$ (**8**),[9] indicating similar metal carbonyl skeletons. The latter complex has, as evidenced by its crystal structure, a sawhorse $(CO)_3RuRu(CO)_3$ metal carbonyl frame bridged by a $\sigma(N)$-μ_2-η^3-$RNC(H)C(H)CR^1$ fragment,[9] just as proposed for **7**. The new N–H bond in **7** gives rise to an absorption in the ν(NH) region at 3302 cm^{-1} (**7c**) or at 3282 cm^{-1} (**7d**). These values are similar to those reported for $FeM(CO)_6[RNC(R^1)C(R^2)N(H)R]$ (M = Fe, Re).[38]

NMR Spectroscopy. The ^1H and ^{13}C NMR data for the reported dinuclear complexes are included in Tables V and VI. The NMR spectrum of $Ru_2(CO)_6[CH_3C{=}C(H)CH_2N\text{-}t\text{-}Bu]$ (**1c**) is temperature-dependent, as are those of the earlier reported analogues **1a,b,d**, indicating the presence of a fluxional enyl–amido ligand in **1c**, whereby C_α oscillates between the two ruthenium centers with $\Delta G^\ddagger \approx 60$ kJ mol^{-1}.[5,6]

In this paper two complexes, **6c** and **6d**, are reported that contain a MAD-yl ligand in the bridging 5e-donating $\sigma(N)$-$\sigma(C)$-$\eta^2(C{=}C)$ bonding mode. This constitutes a new type of coordination for MAD, which can clearly be distinguished from the chelating 3e-donating $\sigma(N)$-$\sigma(C)$ and the bridging 7e-donating $\sigma(N)$-$\sigma(C)$-$\eta^2(C{=}N)$:$\eta^2(C{=}C)$ coordination modes, on the basis of their distinct NMR characteristics. The H_{im} and H_α protons of a MAD-yl ligand in the 3e-donor mode are usually observed in the narrow regions of 7.7–8.0 and 6.4–6.6 ppm, respectively. Upon additional coordination of the entire N=C—C=C π-system to an adjacent ruthenium center in the 7e-bonding mode, both resonances shift to lower frequencies and are usually found between 6.2–7.5 and 5.0–5.7 ppm, respectively. The H_{im} protons of the 5e-donating MAD-yl ligands of **6c** and **6d** are found as doublets (^3J = 2.5 Hz) at 7.85 and 8.02 ppm, respectively, similar to the case for the 3e coordination mode and indicative of merely $\sigma(N)$ coordination of the imine moiety. The $\sigma(C)$-$\eta^2(C{=}C)$ coordination of the vinyl entity in combination with the $\sigma(N)$ coordination of the imine moiety in **6c** and **6d** causes a

(38) Keijsper, J.; Mul, J.; van Koten, G.; Vrieze, K.; Ubbels, H. C.; Stam, C. H. *Organometallics* **1984**, *3*, 1732.

appreciable shielding of the vinyl H_α protons, which are now found near 2.90 ppm, i.e. more than 2 ppm lower compared to the position for the 7e coordination mode. The H_{im} and H_α protons of **6** show mutual ^3J coupling of 2.5 Hz, similar to the case for the 3e and 7e modes. The chemical shifts of the H_α protons of the 5e-donating α,β-unsaturated ketone ligands in the isostructural complexes $HRu_2(CO)_6[C_6H_5C{=}C(H)C(CH_3){=}O]$[26] and $HOs_2(CO)_6[CH_3CH_2C{=}C(H)C(CH_3){=}O]$[27] are observed at 3.51 and 4.06 ppm, respectively, somewhat higher compared to the δ values found for **6c,d**.

The hydrides in **6c,d** resonate at about δ −13.1 ppm, similar to the value reported for $HRu_2(CO)_6[C_6H_5C{=}C(H)C(CH_3){=}O]$ (δ −12.6 ppm), for which the bridging nature of the hydride was established crystallographically.[26,37] A further hint as to the bridging character of the hydride present in **6d** was inferred from the fact that in CCl_4 no rapid H/Cl exchange was observed for **6d**. The appearance of diastereotopic *i*-Pr methyl groups in the ^1H NMR spectrum of **6d** at room temperature indicates a static coordination of the organic ligand to the metal core. The rather high δ value of 3.24 ppm found for the H_γ methyl protons in **6c** might be a consequence of the proximity of one (or both) ruthenium centers. In 3e and 7e MAD-yl ligands this resonance is usually observed in the region of 2.0–2.8 ppm.[3,4,6,30]

The C_{im} and C_α carbon resonances for **6c** are observed at 175.7 and 53.4 ppm and for **6d** at 180.6 and 48.6 ppm, respectively.[5] The δ values of the C_α atoms are about 90 ppm lower when compared to the corresponding free ligand values of about 140 ppm and fall outside the 88–105 ppm region, for C_α resonances of 7e-donating MAD-yl ligands.[3,4,6,30] Thus, both ^1H and ^{13}C NMR data for β-metalated MAD-yl ligands are very useful to determine the coordination mode of the MAD-yl ligand to a metal carbonyl frame. The chemical shifts of the metalated C_β atoms in **6c** and **6d** of 151.4 and 154.1 ppm, respectively, fall just outside the region of 160–200 ppm, where resonances of carbon atoms that are σ-coordinated to one ruthenium center and π-coordinated to another are usually found.[39]

The complexes **7c–e** contain a new variety of an isomerized MAD, a formally 6e-donating dianionic $\sigma(N)$-$\sigma(C_\beta)$-η^3-$R^1C(H)C(H)N(H)R^2$ ligand. The proposed coordination mode of this ligand to the $Ru_2(CO)_6$ core is similar to that of its dehydrogenated counterpart in $Ru_2(CO)_6[C_3H_3CC(H)C(H)N{=}C(CH_3)_2]$ (**8**), which has been characterized by a crystal structure.[9] The former H_{im} and H_α protons in **7** resonate at about 4.3 ppm and 5.62 ($R^1 = CH_3$) or 5.87 ppm ($R^1 = C_6H_5$), respectively, which is in agreement with the present allylic character of the ligand. The H_{im} proton couples with both H_α ($^3J \approx 2.5$ Hz) and the new N–H proton ($^3J \approx 1.5$ Hz); the latter is found as a broad signal at 2.6 (R^2 = *i*-Pr) or 2.8 ppm (R^2 = *t*-Bu). The very small ^3J coupling between the N–H and the *i*-Pr CH protons in **7d** (≤0.5 Hz) indicates that the dihedral angle between the N–H and *i*-Pr C–H bonds is close to 90 °C (Karplus–Conroy relation).

The δ values of the bridging allyl moiety are found at about 170 ppm (μ_2-C_β), 90 ppm (central C), and 57 ppm (terminal C), which values are comparable to those observed for **8** (168.7, 88.3, and 64.8 ppm, respectively).[9] Both the ^1H and ^{13}C NMR spectra of **7d** show diastereotopic *i*-Pr groups, which implies that the chiral N atom is coordinated to a ruthenium center and that the ligand is not involved in a rapid fluxional process (on the NMR time scale).

(39) Aime, A. J.; Milone, L.; Osella, D.; Valle, M.; Randell, E. W. *Inorg. Chim. Acta* **1976**, *20*, 217.

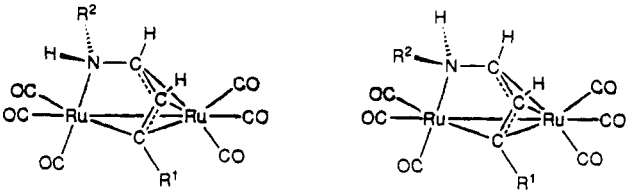

(R_N)-**7** (S_N)-**7**

Figure 5. The two possible diastereomers of **7**.

Since complex **7** contains two independent chiral centers, the N atom and the cyclometalated Ru atom,[22,40] it may exist in two diastereomeric configurations, each of which is represented by one of its enantiomers in Figure 5. However, NMR spectroscopy shows only one set of resonances for the allylamine ligands in **7c–e**, pointing to the presence of only one diastereomer for each. At present the configuration of **7** is not known. We note that also for the isostructural complexes $FeM(CO)_6[RNC(R^1)C(R^2)N(H)R]$ (M = Mn, Re) only one set of resonances was observed in their NMR spectra,[38] indicating, as for **7**, the presence of only one of the two possible geometric isomers.

Discussion

The first product observed during the reaction of (*CA/AC*)-**3a** with H_2 is the hydrido complex **2a**. During this conversion the central intermetallic bond in **3a** is broken and a hydrogen atom is added to each dinuclear metal pentacarbonyl fragment. The 7e coordination mode of the MAD-yl ligand has remained unchanged.

There are three prerequisites for the reaction of a transition-metal (d^8) complex with H_2:[42] (i) low formal oxidation state of the metal, (ii) a site of coordinative unsaturation, and (iii) high basicity of the complex. In linear tetranuclear **3a** prerequisites i and iii are obviously fulfilled, while a free coordination site is apparently easily created during the course of the reaction, since it already proceeds at 40 °C under 1 bar of H_2. In principle three possibilities to create an open site might be considered: (a) loss of CO, (b) fission of the central metal–metal bond, and (c) partial dissociation of the MAD-yl ligand. Loss of CO is unlikely to occur at 40 °C, since **3a** is thermally rather stable,[30b] which would not be expected if labile CO ligands were present. Thermal fission of the central metal–metal bond does occur, but only at elevated temperatures (i.e. above 70 °C),[4] which excludes possibility b. On the basis of the observed hemilability of the 7e MAD-yl ligand in **3a** under an atmosphere of CO,[9] whereby the η^2(C=N):η^2(C=C) π-coordinating systems are stepwise-substituted by CO ligands at ambient temperature, route c is more likely. A similar hemilabile 7e MAD-yl ligand is present in **2**. The η^2(C=N) moiety of the MAD-yl ligand in **2** is readily substituted by a CO ligand at room temperature, affording **6** (vide supra). Thus, a likely route for the present hydrogenation reaction starts with dissociation of the η^2(C=N) π-bond, thereby creating a 16e ruthenium center, thus providing a reactive site for incoming ligands (such as H_2). Next, the H_2 molecule is oxidatively added to the cluster core forming the *cis*-dihydride **10a**. Finally,

(40) We note that the other ruthenium atom is chiral as well. Its chirality, however, is directly related to that of the cyclometalated ruthenium atom.

(41) Reference deleted in revision.

(42) (a) Deeming, A. J. In *Transition Metal Clusters*; Johnson, B. F. G., Ed.; Wiley-Interscience: Chichester, England, 1980; p 391. (b) Vahrenkamp, H. *Adv. Organomet. Chem.* **1983**, *22*, 169. (c) Keijsper, J.; Polm, L. H.; van Koten, G.; Vrieze, K.; Nielsen, E.; Stam, C. H. *Organometallics* **1985**, *4*, 2006. (d) Keijsper, J.; Polm, L. H.; van Koten, G.; Vrieze, K.; Nielsen, E.; Stam, C. H. *Organometallics* **1985**, *3*, 438.

Scheme V. Proposed Reaction Steps during the Hydrogenation of the Two Diastereomers of 3a at 40 °C

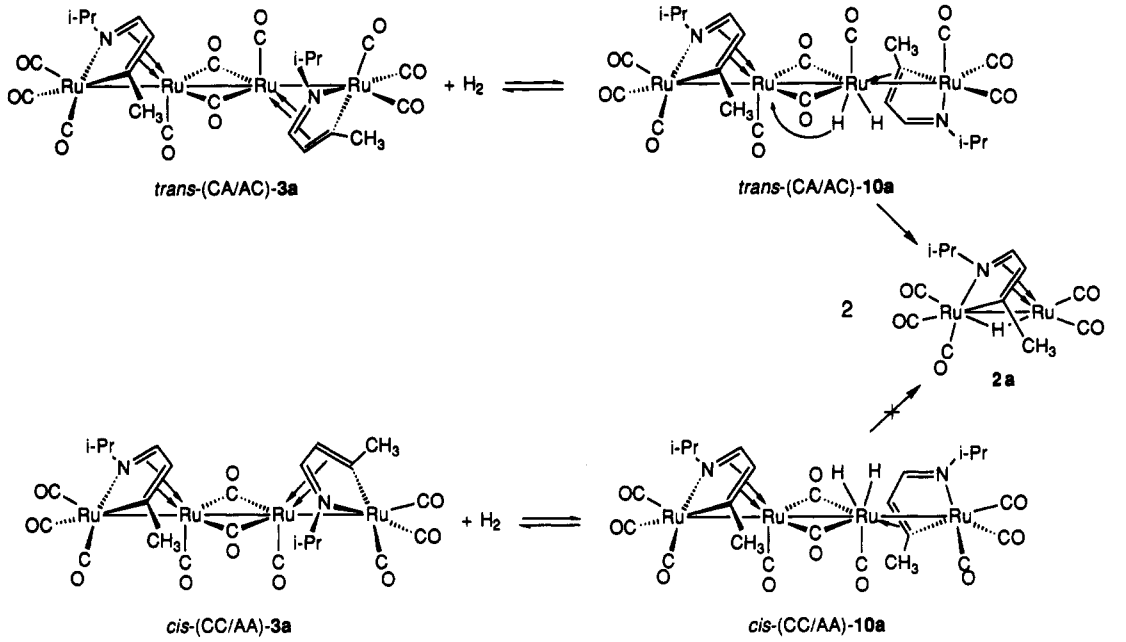

migration of one of these hydrides to the adjacent central ruthenium center with concomitant breaking of the central intermetallic bond and recoordination of the dissociated C=N group lead to the formation of two molecules of **2a**.

The more facile reaction of H_2 with (*CA/AC*)-**3a** compared to that with (*CC/AA*)-**3a** is of particular interest, because this difference in reactivity may be explored in various diastereoselective syntheses. Bearing in mind the mechanism proposed above, the π-C=N moieties in (*CC/AA*)-**3a** seem to be more strongly bonded to the cluster core compared to those of (*CA/AC*)-**3a**. Both diastereomers of **3a** have been characterized crystallographically (i.e. the trans-*CC/AA* and cis-*CA/AC* isomers of **3a**), but it has been shown that in solution (NMR) as well as in the solid state (IR) both the cis and trans diastereomers may be present. On the basis of the four structural isomers of **3a**, a likely answer may be provided with respect to the observed different kinetic barriers of the *CC/AA* and *CA/AC* diastereomers of **3a** toward reactions with H_2. As has been elaborated elsewhere,[4] the Ru–π-C=N bonds of the various geometric isomers will differ somewhat in strength due to the coordination of either *both* π-bonded imines trans to one of the bridging CO ligands (as in *cis*-(*CA/AC*)-**3a** and *trans*-(*CC/AA*)-**3a**) or coordination of *one* π-bonded imine and *one* π-bonded olefin trans to one of the bridging CO ligands (as in *trans*-(*CA/AC*)-**3a** and *cis*-(*CC/AA*)-**3a**). In the former geometries, the Ru–π-C=N bonds will be somewhat stronger due to enhanced π back-bonding to the π^* orbitals of these imine moieties compared to the latter. More facile dissociation of C=N and hence more facile addition of H_2 to the cluster core is therefore likely to take place in *cis*-(*CC/AA*)-**3a** and *trans*-(*CA/AC*)-**3a**, the isomers observed in the crystal structures, compared to *trans*-(*CC/AA*)-**3a** and *cis*-(*CA/AC*)-**3a**. Oxidative addition of H_2 to the former isomers results in the formation of the *cis*-dihydrides *cis*-(*CC/AA*)-**10a** and *trans*-(*CA/AC*)-**10a**, as shown in Scheme V. The different relative positions of the hydrides and the still 7e-donating MAD-yl ligands in the two H_2 adducts are interesting. In *cis*-(*CC/AA*)-**10a** the ligands would be bonded to the same side of the cluster core, whereas in *trans*-(*CA/AC*)-**10a** they are bonded to opposite sides. The crystal structure of $HRu_2(CO)_5$-[C_6H_5C=C(H)C(H)=N-*i*-Pr] (**2d**) shows the μ-H in a position trans to the MAD-yl ligand. Migration of one of the hydrides in the H_2 adducts with concomitant fission of the central Ru–Ru bond, which would result in the formation of two molecules of **2a**, is more facile in *trans*-(*CA/AC*)-**10a** than in *cis*-(*CC/AA*)-**10a**, since the hydrides in the former are located at a position from which migration to the other part of the cluster is easy to conceive. In *cis*-(*CC/AA*)-**10a**, the hydrides are positioned at the "wrong side" of the cluster to be transferred to a position trans to the MAD-yl ligand at the other half of the molecule and instead reductive elimination of H_2 is more likely to occur. Thus, at 40 °C (*CA/AC*)-**3a** reacts with H_2 to give two molecules of **2a**, whereas (*CC/AA*)-**3a** will also react with H_2, but reductive elimination of the two hydrides from its initial hydrogenation product *cis*-(*CC/AA*)-**10a** to give (*CC/AA*)-**3a** is favored, and no net reaction takes place. At higher temperatures (70 °C) (*CC/AA*)-**3a** also reacts with H_2 to give **2a**, probably because then effective H_2 addition takes place to the trans-(*CC/AA*) isomer and, since the two hydrides are located at the side opposite to the 7e MAD-yl ligand, also migration of one of these hydrides to the other part of the cluster and, hence, cluster breakdown may take place.

For both clusters **3a** and **5a** the *CA/AC* diastereomers appear to be more reactive toward H_2. The relative instability of (*CA/AC*)-**5a** compared to (*CC/AA*)-**5a** might have a steric cause. Molecular graphics studies of (*CA/AC*)-**5a**, which has been generated by substitution of C(2)–C(1)H_3 for an N-*i*-Pr group and N(1)-*i*-Pr for a C–CH_3 group in (*CC/AA*)-**5a** (see Figure 3), have shown that a CH_3 group of the introduced N-*i*-Pr group in (*CA/AC*)-**5a** is very close to either C(21)–O(7) or C(18)–O(4); hence, the instability of (*CC/AA*)-**5a** might well be steric in origin. Another possibility for its instability might be the relative orientations of the two hydrides with respect to the MAD-yl ligands. In (*CC/AA*)-**5a** both hydrides occupy bridging positions which are trans to a C atom and cis to a N atom of the σ(N)-σ(C)-coordinated part of the MAD-yl ligand. In (*CA/AC*)-**5a**, one of the hydrides occupies a similar position, but the other is in a position cis to a C atom and trans to a N atom. The cis position of the hydride with respect to the C atom might result in the facile

Scheme VI. Directable H-Transfer Reactions in $HRu_2(CO)_6[R^1C{=}C(H)C(H){=}NR^2]$ (6) Giving either $Ru_2(CO)_6[R^1C{=}C(H)CH_2NR^2]$ (1) or $Ru_2(CO)_6[R^1CC(H)C(H)N(H)R^2]$ (7)

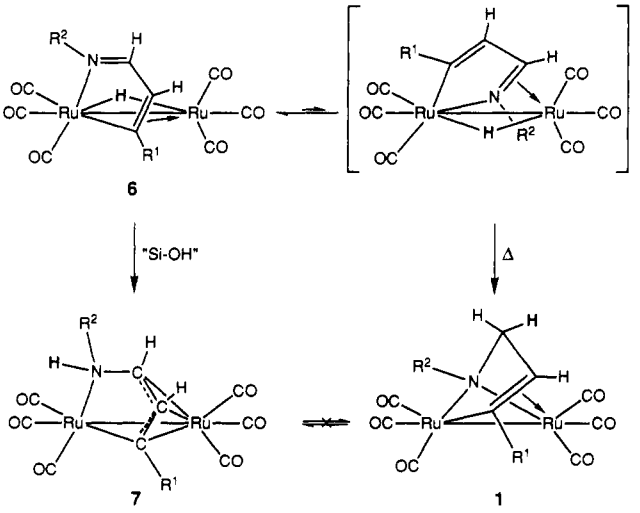

reductive elimination of $C_\beta H$, after which further hydrogenations become feasible and ultimately result in the complete breakdown of (*CA/AC*)-**5a**, yielding $H_4Ru_4(CO)_{12}$ and (*n*-Bu)N(H)(*i*-Pr).

Hydrogenation of $Ru_2(CO)_6[CH_2CC(H)C(H){=}NR^2]$ (R^2 = *i*-Pr (**4a**), *t*-Bu (**4c**)) may well proceed via η^3–η^1 slippage of the allyl moiety, thus creating a reactive 16e ruthenium center, to which oxidative addition of H_2 is feasible. Reductive elimination of the $[CH_3]_\gamma$ group then yields **6**, from which further reactions take place, yielding either **1** (R^2 = *i*-Pr) or **3** (R^2 = *t*-Bu). Similar hydrogenations, converting the terminal methylene moiety of an η^3-allyl function into a methyl whereas the other hydrogen atom ends up as a μ-hydride, are known.[43] The decreased reactivity of **4** in the case where R^2 = *t*-Bu might be a consequence of the sterically more demanding properties of the R^2 substituent, thereby shielding the open site on the metal core of the η^1-allyl intermediate and hampering incoming ligand (e.g. H_2) attack.

Transfer of the hydride ligand to the imine C atom during the thermal isomerization of **6** into **1** is considerably more facile in case the R^2 substituent is an *i*-Pr group instead of the more bulky *t*-Bu group. Bearing this in mind, a likely mechanism for the H transfer of the metal core to the imine C atom may be provided. Direct H transfer seems unlikely since the parent hydride **6** has to be heated to induce the H transfer (Scheme VI) and, furthermore, direct H transfer does not account for the observed R^2 substituent dependence of the isomerization. We propose that prior to H transfer the coordination mode of the 5e MAD-yl ligand changes from σ(N)-σ(C)-η^2(C=C) to σ(N)-σ(C)-η^2(C=N), as shown in Scheme VI. Now the imine C atom is directly coordinated to the metal core and transfer of the bridging hydride to this C atom is feasible.[44] This mechanism also provides an explanation for the observed R^2 substituent dependence of this isomerization, as the η^2(C=N) bonding mode will be destabilized when R^2 is a bulky *t*-Bu group.

In compound **7**, which is formed by a silica-induced isomerization of **6**, the hydride has formally been transferred to the N atom instead of to the C atom of the imine moiety. Alternatively, however, the H atom may have been abstracted as a proton from the silica catalyst (a Brønsted acid). The latter possibility seems more likely, since not even the slightest amount of **7** is formed during the thermal isomerization of **6**. This isomerization shows that silica may induce chemical conversions in organometallic systems which are not available or difficult to achieve by alternative chemical methods.[45]

Acknowledgment. We thank Prof. G. van Koten and Dr. H.-W. Frühauf for helpful discussions, J.-M. Ernsting for recording the 62.9-MHz ^{13}C NMR spectrum, and G. U-A-Sai and R. Fokkens for the mass spectra. This research was supported by the Netherlands Foundation for Chemical Research (SON), with financial aid from the Netherlands Organization for Scientific Research (NWO).

Supplementary Material Available: Tables of the anisotropic thermal parameters of the non-H atoms, the calculated fractional coordinates and the isotropic thermal parameters of the H atoms, and all bond distances and angles (5 pages); a listing of the structure factor amplitudes (39 pages). Ordering information is given on any current masthead page.

OM910635U

(43) (a) Castiglioni, M.; Milone, L.; Vaglio, G. A.; Osella, D.; Valle, M. *Inorg. Chem.* **1976**, *15*, 394. (b) Nucciarone, D.; Taylor, N. J.; Carty, A. J. *Organometallics* **1988**, *7*, 127.

(44) Fryzuk, M. D.; Piers, W. E. *Organometallics* **1990**, *9*, 986.

(45) (a) Holton, R. A.; Nelson, R. V. *J. Organomet. Chem.* **1980**, *201*, C35. (b) Simms, B. L.; Shang, M.; Youngs, J. L.; Ibers, J. A. *Organometallics* **1987**, *6*, 1118.